

CERN-PH-EP-2014-043

Submitted to: Physical Review D

Flavour tagged time dependent angular analysis of the $B_s^0 \rightarrow J/\psi\phi$ decay and extraction of $\Delta\Gamma_s$ and the weak phase ϕ_s in ATLAS

The ATLAS Collaboration

Abstract

A measurement of the $B_s^0 \rightarrow J/\psi\phi$ decay parameters, updated to include flavour tagging is reported using 4.9 fb^{-1} of integrated luminosity collected by the ATLAS detector from $\sqrt{s} = 7 \text{ TeV}$ pp collisions recorded in 2011 at the LHC. The values measured for the physical parameters are:

$$\begin{aligned}\phi_s &= 0.12 \pm 0.25 \text{ (stat.)} \pm 0.05 \text{ (syst.) rad} \\ \Delta\Gamma_s &= 0.053 \pm 0.021 \text{ (stat.)} \pm 0.010 \text{ (syst.) ps}^{-1} \\ \Gamma_s &= 0.677 \pm 0.007 \text{ (stat.)} \pm 0.004 \text{ (syst.) ps}^{-1} \\ |A_{\parallel}(0)|^2 &= 0.220 \pm 0.008 \text{ (stat.)} \pm 0.009 \text{ (syst.)} \\ |A_0(0)|^2 &= 0.529 \pm 0.006 \text{ (stat.)} \pm 0.012 \text{ (syst.)} \\ \delta_{\perp} &= 3.89 \pm 0.47 \text{ (stat.)} \pm 0.11 \text{ (syst.) rad}\end{aligned}$$

where the parameter $\Delta\Gamma_s$ is constrained to be positive. The S -wave contribution was measured and found to be compatible with zero. Results for ϕ_s and $\Delta\Gamma_s$ are also presented as 68% and 95% likelihood contours, which show agreement with the Standard Model expectations.

Flavour tagged time dependent angular analysis of the $B_s^0 \rightarrow J/\psi\phi$ decay and extraction of $\Delta\Gamma_s$ and the weak phase ϕ_s in ATLAS

The ATLAS Collaboration

(Dated: July 8, 2014)

A measurement of the $B_s^0 \rightarrow J/\psi\phi$ decay parameters, updated to include flavour tagging is reported using 4.9 fb^{-1} of integrated luminosity collected by the ATLAS detector from $\sqrt{s} = 7$ TeV pp collisions recorded in 2011 at the LHC. The values measured for the physical parameters are:

$$\begin{aligned}\phi_s &= 0.12 \pm 0.25 \text{ (stat.)} \pm 0.05 \text{ (syst.) rad} \\ \Delta\Gamma_s &= 0.053 \pm 0.021 \text{ (stat.)} \pm 0.010 \text{ (syst.) ps}^{-1} \\ \Gamma_s &= 0.677 \pm 0.007 \text{ (stat.)} \pm 0.004 \text{ (syst.) ps}^{-1} \\ |A_{\parallel}(0)|^2 &= 0.220 \pm 0.008 \text{ (stat.)} \pm 0.009 \text{ (syst.)} \\ |A_0(0)|^2 &= 0.529 \pm 0.006 \text{ (stat.)} \pm 0.012 \text{ (syst.)} \\ \delta_{\perp} &= 3.89 \pm 0.47 \text{ (stat.)} \pm 0.11 \text{ (syst.) rad}\end{aligned}$$

where the parameter $\Delta\Gamma_s$ is constrained to be positive. The S -wave contribution was measured and found to be compatible with zero. Results for ϕ_s and $\Delta\Gamma_s$ are also presented as 68% and 95% likelihood contours, which show agreement with the Standard Model expectations.

I. INTRODUCTION

New phenomena beyond the predictions of the Standard Model (SM) may alter CP violation in B -decays. A channel that is expected to be sensitive to new physics contributions is the decay $B_s^0 \rightarrow J/\psi\phi$. CP violation in the $B_s^0 \rightarrow J/\psi\phi$ decay occurs due to interference between direct decays and decays with $B_s^0 - \bar{B}_s^0$ mixing. The oscillation frequency of B_s^0 meson mixing is characterized by the mass difference Δm_s of the heavy (B_H) and light (B_L) mass eigenstates. The CP violating phase ϕ_s is defined as the weak phase difference between the $B_s^0 - \bar{B}_s^0$ mixing amplitude and the $b \rightarrow c\bar{c}s$ decay amplitude. In the absence of CP violation, the B_H state would correspond to the CP odd state and the B_L to the CP even state. In the SM the phase ϕ_s is small and can be related to CKM quark mixing matrix elements via the relation $\phi_s \simeq -2\beta_s$, with $\beta_s = \arg[-(V_{ts}V_{tb}^*)/(V_{cs}V_{cb}^*)]$; a value of $\phi_s \simeq -2\beta_s = -0.037 \pm 0.002$ rad [1] is predicted in the SM. Many new physics models predict large ϕ_s values whilst satisfying all existing constraints, including the precisely measured value of Δm_s [2, 3].

Another physical quantity involved in $B_s^0 - \bar{B}_s^0$ mixing is the width difference $\Delta\Gamma_s = \Gamma_L - \Gamma_H$, which is predicted to be $\Delta\Gamma_s = 0.087 \pm 0.021$ ps $^{-1}$ [4]. Physics beyond the SM is not expected to affect $\Delta\Gamma_s$ as significantly as ϕ_s [5]. Extracting $\Delta\Gamma_s$ from data is nevertheless useful as it allows theoretical predictions to be tested [5].

The decay of the pseudoscalar B_s^0 to the vector–vector final-state $J/\psi\phi$ results in an admixture of CP odd and CP even states, with orbital angular momentum $L = 0, 1$ or 2 . The final states with orbital angular momentum $L = 0$ or 2 are CP even while the state with $L = 1$ is CP odd. Flavour tagging is used to distinguish between the initial B_s^0 and \bar{B}_s^0 states. The CP states are separated statistically using an angular analysis of the final-state

particles.

In this paper, an update to the previous measurement [6] with the addition of flavour tagging, is presented. Flavour tagging significantly reduces the uncertainty of the measured value of ϕ_s while also allowing a measurement of one of the strong phases. Previous measurements of these quantities have been reported by the DØ, CDF and LHCb collaborations [7–9]. The analysis presented here uses 4.9 fb^{-1} of LHC pp data at $\sqrt{s} = 7$ TeV collected by the ATLAS detector in 2011.

II. ATLAS DETECTOR AND MONTE CARLO SIMULATION

The ATLAS experiment [10] is a multipurpose particle physics detector with a forward-backward symmetric cylindrical geometry and near 4π coverage in solid angle. The inner tracking detector (ID) consists of a silicon pixel detector, a silicon microstrip detector and a transition radiation tracker. The ID is surrounded by a thin superconducting solenoid providing a 2 T axial magnetic field, and by a high granularity liquid-argon sampling electromagnetic calorimeter. A steel/scintillator tile calorimeter provides hadronic coverage in the central rapidity range. The end-cap and forward regions are instrumented with Liquid-argon calorimeters for both electromagnetic and hadronic measurements. The muon spectrometer (MS) surrounds the calorimeters and consists of three large superconducting toroids with eight coils each, a system of tracking chambers, and detectors for triggering.

The muon and tracking systems are of particular importance in the reconstruction of B meson candidates. Only data where both systems were operating correctly and where the LHC beams were declared to be stable are used. A muon identified using a combination of MS and ID track parameters is referred to as *combined*. A

muon formed by track segments which are not associated with an MS track, but which are matched to ID tracks extrapolated to the MS is referred to as *segment tagged*.

The data were collected during a period of rising instantaneous luminosity, and the trigger conditions varied over this time. The triggers used to select events for this analysis are based on identification of a $J/\psi \rightarrow \mu^+\mu^-$ decay, with either a 4 GeV transverse momentum [11] (p_T) threshold for each muon or an asymmetric configuration that applies a p_T threshold of 4 GeV to one of the muons while accepting a second muon with p_T as low as 2 GeV.

Monte Carlo (MC) simulation is used to study the detector response, estimate backgrounds and model systematic effects. For this study, 12 million MC-simulated $B_s^0 \rightarrow J/\psi\phi$ events were generated using PYTHIA 6 [12] tuned with recent ATLAS data [13]. No p_T cuts were applied at the generator level. Detector responses for these events were simulated using the ATLAS simulation package based on GEANT4 [14, 15]. Pile-up corresponding to the conditions during data taking was included. In order to take into account the varying trigger configurations during data-taking, the MC events were weighted to have the same trigger composition as the collected collision data. Additional samples of the background decay $B^0 \rightarrow J/\psi K^{0*}$ as well as the more general $bb \rightarrow J/\psi X$ and $pp \rightarrow J/\psi X$ backgrounds were also simulated using PYTHIA.

III. RECONSTRUCTION AND CANDIDATE SELECTION

Events passing the trigger and the data quality selections described in section II are required to pass the following additional criteria: the event must contain at least one reconstructed primary vertex, built from at least four ID tracks, and at least one pair of oppositely charged muon candidates that are reconstructed using information from the MS and the ID [16]. Both combined and segment tagged muons are used. In this analysis the muon track parameters are taken from the ID measurement alone, since the precision of the measured track parameters for muons in the p_T range of interest for this analysis is dominated by the ID track reconstruction. The pairs of muon tracks are refitted to a common vertex and accepted for further consideration if the fit results in $\chi^2/\text{d.o.f.} < 10$. The invariant mass of the muon pair is calculated from the refitted track parameters. To account for varying mass resolution, the J/ψ candidates are divided into three subsets according to the pseudorapidity η of the muons. A maximum likelihood fit is used to extract the J/ψ mass and the corresponding resolution for these three subsets. When both muons have $|\eta| < 1.05$, the dimuon invariant mass must fall in the range (2.959–3.229) GeV to be accepted as a J/ψ candidate. When one muon has $1.05 < |\eta| < 2.5$ and the other muon $|\eta| < 1.05$, the corresponding signal region is (2.913–3.273) GeV. For the third subset, where both

muons have $1.05 < |\eta| < 2.5$, the signal region is (2.852–3.332) GeV. In each case the signal region is defined so as to retain 99.8% of the J/ψ candidates identified in the fits.

The candidates for $\phi \rightarrow K^+K^-$ are reconstructed from all pairs of oppositely charged particles with $p_T > 0.5$ GeV and $|\eta| < 2.5$ that are not identified as muons. Candidates for $B_s^0 \rightarrow J/\psi(\mu^+\mu^-)\phi(K^+K^-)$ are sought by fitting the tracks for each combination of $J/\psi \rightarrow \mu^+\mu^-$ and $\phi \rightarrow K^+K^-$ to a common vertex. Each of the four tracks is required to have at least one hit in the pixel detector and at least four hits in the silicon microstrip detector. The fit is further constrained by fixing the invariant mass calculated from the two muon tracks to the J/ψ mass [17]. These quadruplets of tracks are accepted for further analysis if the vertex fit has a $\chi^2/\text{d.o.f.} < 3$, the fitted p_T of each track from $\phi \rightarrow K^+K^-$ is greater than 1 GeV and the invariant mass of the track pairs (under the assumption that they are kaons) falls within the interval $1.0085 \text{ GeV} < m(K^+K^-) < 1.0305 \text{ GeV}$. If there is more than one accepted candidate in the event, the candidate with the lowest $\chi^2/\text{d.o.f.}$ is selected. In total 131513 B_s^0 candidates are collected within a mass range of $5.15 < m(B_s^0) < 5.65 \text{ GeV}$.

For each B_s^0 meson candidate the proper decay time t is estimated by the expression:

$$t = \frac{L_{xy} M_B}{p_{T_B}},$$

where p_{T_B} is the reconstructed transverse momentum of the B_s^0 meson candidate and M_B denotes the world average mass value [17] of the B_s^0 meson. The transverse decay length, L_{xy} , is the displacement in the transverse plane of the B_s^0 meson decay vertex with respect to the primary vertex, projected onto the direction of the B_s^0 transverse momentum. The position of the primary vertex used to calculate this quantity is refitted following the removal of the tracks used to reconstruct the B_s^0 meson candidate.

For the selected events the average number of pileup interactions is 5.6, necessitating a choice of the best candidate for the primary vertex at which the B_s^0 meson is produced. The variable used is the three-dimensional impact parameter d_0 , which is calculated as the distance between the line extrapolated from the reconstructed B_s^0 meson vertex in the direction of the B_s^0 momentum, and each primary vertex candidate. The chosen primary vertex is the one with the smallest d_0 . Using MC simulation it is shown that the fraction of B_s^0 candidates which are assigned the wrong primary vertex is less than 1% and that the corresponding effect on the final results is negligible. No B_s^0 meson decay time cut is applied in the analysis.

IV. FLAVOUR TAGGING

The determination of the initial flavour of neutral B -mesons can be inferred using information from the B -meson that is typically produced from the other b -quark in the event [18]. This is referred to as the opposite-side tagging (OST).

To study and calibrate the OST methods, events containing the decays of $B^\pm \rightarrow J/\psi K^\pm$ can be used, where flavour of the B -meson at production is provided by the kaon charge. Events from the entire 2011 run period satisfying the same data quality selections as described in section 2 are used.

A. $B^\pm \rightarrow J/\psi K^\pm$ event selection

To be selected for use in the calibration analysis, events must satisfy a trigger condition requiring two oppositely charged muons within an invariant mass range around the nominal J/ψ mass. Candidate $B^\pm \rightarrow J/\psi K^\pm$ decays are identified using two oppositely charged combined muons forming a good vertex using information supplied by the inner detector. Each muon is required to have a transverse momentum of at least 4 GeV and pseudo-rapidity within $|\eta| < 2.5$. The invariant mass of the dimuon candidate is required to satisfy $2.8 < m(\mu^+\mu^-) < 3.4$ GeV. To form the B candidate an additional track with the charged kaon mass hypothesis, $p_T > 1$ GeV and $|\eta| < 2.5$ is combined with the dimuon candidate and a vertex fit is performed with the mass of the di-muon pair constrained to the known value of the J/ψ mass. To reduce the prompt component of the combinatorial background, the requirement $L_{xy} > 0.1$ mm is applied to the B candidate. The choice of primary vertex is determined using the same procedure as done for the B_s^0 candidates.

In order to study the distributions corresponding to the signal processes with the background component removed, a sideband subtraction method is defined. Events are separated into five equal regions of B candidate rapidity from $0 - 2.5$ and three mass regions. The mass regions are defined as a signal region around the fitted peak signal mass position $\mu \pm 2\sigma$ and the sidebands are $[\mu - 5\sigma, \mu - 3\sigma]$ and $[\mu + 3\sigma, \mu + 5\sigma]$, where μ and σ are the mean and width of the Gaussian function describing the B signal mass, for each rapidity region. Individual binned extended maximum likelihood fits to the invariant mass distribution are performed in each region of rapidity.

The background is modelled by an exponential to describe combinatorial background and a hyperbolic tangent function to parameterize the low-mass contribution from incorrectly or partially reconstructed B decays. A Gaussian function is used to model the $B^\pm \rightarrow J/\psi \pi^\pm$ contribution. The contributions of non-combinatorial backgrounds are found to have a negligible effect in the tagging procedure. Figure 1 shows the invariant mass

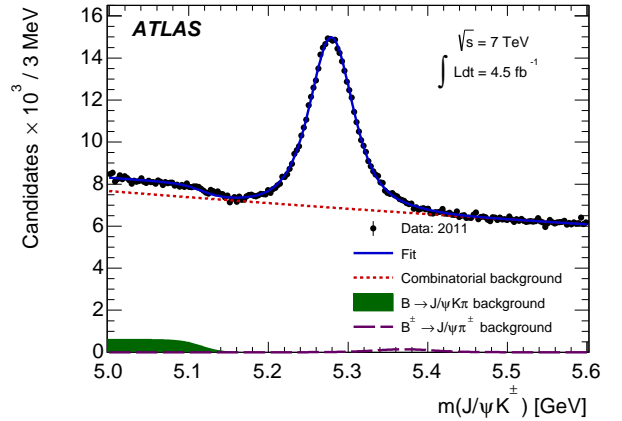


FIG. 1. The invariant mass distribution for $B^\pm \rightarrow J/\psi K^\pm$ candidates. Included in this plot are all events passing the selection criteria. The data are shown by points, and the overall result of the fit is given by the blue curve. The combinatorial background component is given by the red dotted line, partially reconstructed B decays by the green shaded area, and decays of $B^\pm \rightarrow J/\psi \pi^\pm$, where the pion is mis-assigned a kaon mass by a purple dashed line.

distribution of B candidates for all rapidity regions overlaid with the fit result for the combined data.

B. Tagging methods

Several methods are available to infer the flavour of the opposite-side b -quark, with varying efficiencies and discriminating powers. The measured charge of a muon from the semileptonic decay of the B meson provides strong separation power; however, the $b \rightarrow \mu$ transitions are diluted through neutral B meson oscillations, as well as by cascade decays $b \rightarrow c \rightarrow \mu$ which can alter the sign of the muon relative to the one from direct semileptonic decays $b \rightarrow \mu$. The separation power of tagging muons can be enhanced by considering a weighted sum of the charge of the tracks in a cone around the muon. If no muon is present, a weighted sum of the charge of tracks associated with the opposite-side B meson decay will provide some separation. The tagging methods are described in detail below.

For muon-based tagging, an additional muon is required in the event, with $p_T > 2.5$ GeV, $|\eta| < 2.5$ and with $|\Delta z| < 5$ mm from the primary vertex. Muons are classified according to their reconstruction class, *combined* or *segment tagged*, and subsequently treated as distinct tagging methods. In the case of multiple muons, the muon with highest transverse momentum is selected.

A muon *cone charge* variable is constructed, defined as

$$Q_\mu = \frac{\sum_i^{N \text{ tracks}} q_i \cdot (p_T^i)^\kappa}{\sum_i^{N \text{ tracks}} (p_T^i)^\kappa},$$

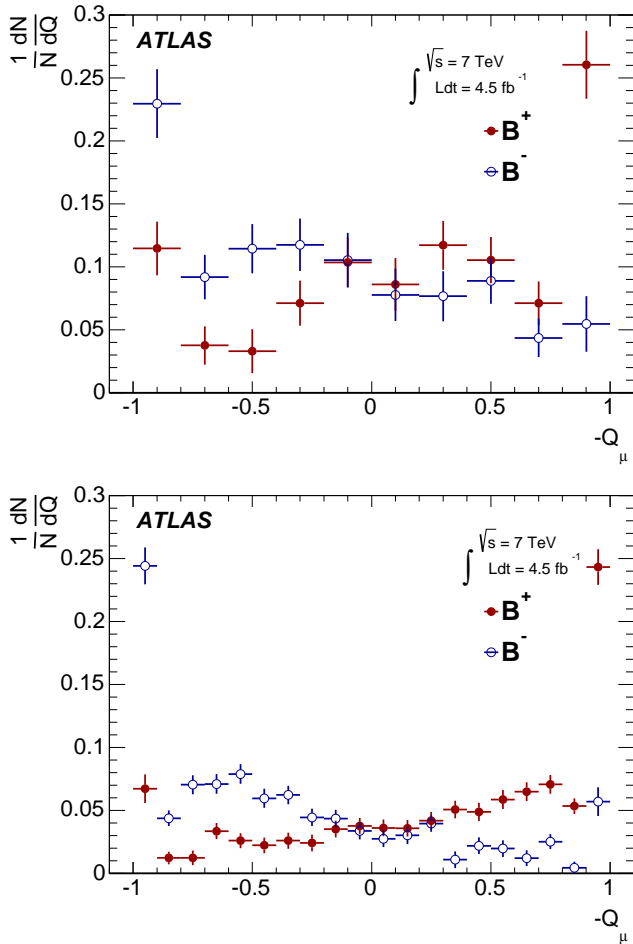


FIG. 2. The opposite-side muon cone charge distribution for B^\pm signal candidates for *segment tagged* (top) and *combined* (bottom) muons.

where q is the charge of the track, $\kappa = 1.1$ and the sum is performed over the reconstructed ID tracks within a cone size of $\Delta R = 0.5$ [19] around the muon direction and the muon track is included as well. The reconstructed ID tracks must have a $p_T > 0.5$ GeV and $|\eta| < 2.5$. The value of the parameter κ was determined while optimizing the tagging performance. Tracks associated with the signal decay are explicitly excluded from the sum. In figure 2 the opposite-side muon cone charge distributions are shown for candidates from B^\pm signal decays. In the absence of a muon, a b-tagged jet [20] is required in the event, which is seeded from calorimeter clusters, with minimum energy threshold of 10 GeV, and where a minimum b-tag weight requirement of at least -0.5 is applied. The jet tracks are required to be associated with the same primary vertex as the signal decay, excluding those from the signal candidate. Jets within a cone of $\Delta R < 0.5$ of the signal momentum axis are excluded. The jet is reconstructed using the anti- k_t algorithm with a cone size of 0.6. In the case of multiple jets, the jet

with the highest value of the b -tag weight is used.

A *jet charge* is defined as

$$Q_{\text{jet}} = \frac{\sum_i^N \text{tracks } q^i \cdot (p_T^i)^\kappa}{\sum_i^N \text{tracks } (p_T^i)^\kappa},$$

where $\kappa = 1.1$, and the sum is over the tracks associated with the jet, using the method described in ref. [21]. Figure 3 shows the distribution of charges for opposite-side jet charge from B^\pm signal candidate events.

The efficiency ϵ of an individual tagger is defined as the ratio of the number of tagged events to the total number of candidates. A probability that a specific event has a signal decay containing a \bar{b} -quark given the value of the discriminating variable $P(B|Q)$ is constructed from the calibration samples for each of the B^+ and B^- samples, defining $P(Q|B^+)$ and $P(Q|B^-)$ respectively. The probability to tag a signal event as containing a \bar{b} -quark is therefore $P(B|Q) = P(Q|B^+) / (P(Q|B^+) + P(Q|B^-))$ and $P(\bar{B}|Q) = 1 - P(B|Q)$. The tagging power is defined as $\epsilon \mathcal{D}^2 = \sum_i \epsilon_i \cdot (2P_i(B|Q_i) - 1)^2$, where the sum is over the bins of the probability distribution as a function of the charge variable and ϵ_i is the number of tagged events in each bin divided by the total number of candidates. An effective dilution \mathcal{D} is calculated from the tagging power and the efficiency.

The combination of the tagging methods is applied according to the hierarchy of performance, based on the dilution of the tagging method. The single best performing tagging measurement is taken, according to the order: *combined* muon cone charge, *segment tagged* muon cone charge, jet charge. If it is not possible to provide a tagging response for the event, then a probability of 0.5 is assigned. A summary of the tagging performance is given in table 1.

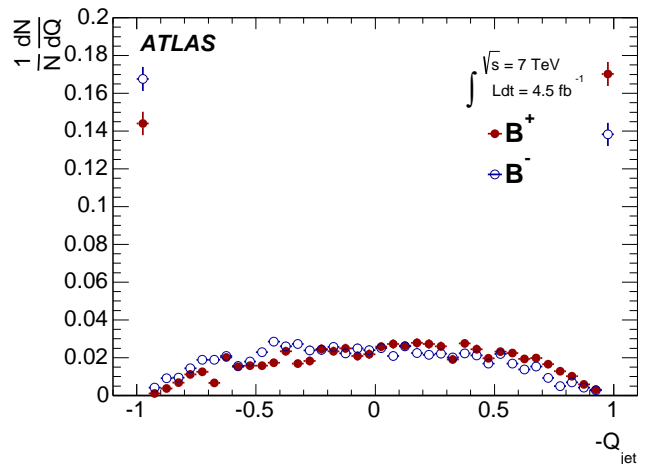


FIG. 3. Jet-charge distribution for B^\pm signal candidates.

Tagger	Efficiency [%]	Dilution [%]	Tagging Power [%]
Combined μ	3.37 ± 0.04	50.6 ± 0.5	0.86 ± 0.04
Segment Tagged μ	1.08 ± 0.02	36.7 ± 0.7	0.15 ± 0.02
Jet charge	27.7 ± 0.1	12.68 ± 0.06	0.45 ± 0.03
Total	32.1 ± 0.1	21.3 ± 0.08	1.45 ± 0.05

TABLE I. Summary of tagging performance for the different tagging methods described in the text. Uncertainties shown are statistical only. The efficiency and tagging power are each determined by summing over the individual bins of the charge distribution. The effective dilution is obtained from the measured efficiency and tagging power. The uncertainties are determined by combining the appropriate uncertainties on the individual bins of each charge distribution.

V. MAXIMUM LIKELIHOOD FIT

An unbinned maximum likelihood fit is performed on the selected events to extract the parameters of the $B_s^0 \rightarrow J/\psi(\mu^+\mu^-)\phi(K^+K^-)$ decay. The fit uses information about the reconstructed mass m and its uncertainty σ_m , the measured proper decay time t and its uncertainty σ_t , the tag probability, and the transversity angles Ω of each $B_s^0 \rightarrow J/\psi\phi$ decay candidate. There are three transversity angles; $\Omega = (\theta_T, \psi_T, \phi_T)$ and these are defined in section V A.

The likelihood function is defined as a combination of the signal and background probability density functions as follows:

$$\ln \mathcal{L} = \sum_{i=1}^N \{ w_i \cdot \ln(f_s \cdot \mathcal{F}_s(m_i, t_i, \Omega_i, P(B|Q))) + f_s \cdot f_{B^0} \cdot \mathcal{F}_{B^0}(m_i, t_i, \Omega_i, P(B|Q)) + (1 - f_s \cdot (1 + f_{B^0})) \cdot \mathcal{F}_{\text{bkg}}(m_i, t_i, \Omega_i, P(B|Q)) \} \quad (1)$$

where N is the number of selected candidates, w_i is a weighting factor to account for the trigger efficiency, f_s is the fraction of signal candidates, f_{B^0} is the fraction of B^0 ($B^0 \rightarrow J/\psi K^{0*}$ and $B^0 \rightarrow J/\psi K^{\pm}\pi^{\mp}$) mesons mis-identified as B_s^0 candidates calculated relative to the number of signal events; this parameter is fixed in the likelihood fit. The mass m_i , the proper decay time t_i and the decay angles Ω_i are the values measured from the data for each event i . \mathcal{F}_s , \mathcal{F}_{B^0} and \mathcal{F}_{bkg} are the probability density functions (PDF) modelling the signal, the specific B^0 background and the other background distributions, respectively. A detailed description of the signal PDF terms in equation (1) is given in section V A. The two background functions are, with the exception of new terms dependent on $P(B|Q)$ which are explained in section V B, unchanged from the previous analysis [6]. They are each described by the product of eight terms which describe the distribution of each measured parameter. With the exception of the lifetime and its uncertainty the background parameters are assumed uncorrelated.

A. Signal PDF

The PDF describing the signal events, \mathcal{F}_s , has the form of a product of PDFs for each quantity measured from the data:

$$\begin{aligned} \mathcal{F}_s(m_i, t_i, \Omega_i, P(B|Q)) = & P_s(m_i, \sigma_{m_i}) \cdot P_s(\sigma_{m_i}) \\ & \cdot P_s(\Omega_i, t_i, P(B|Q), \sigma_{t_i}) \cdot P_s(\sigma_{t_i}) \\ & \cdot P_s(P(B|Q)) \\ & \cdot A(\Omega_i, p_{T_i}) \cdot P_s(p_{T_i}) \end{aligned}$$

The terms $P_s(m_i, \sigma_{m_i})$, $P_s(\Omega_i, t_i, P(B|Q), \sigma_{t_i})$ and $A(\Omega_i, p_{T_i})$ are explained in the current section. The tagging probability term $P_s(P(B|Q))$ is described in section V B. The remaining probability terms $P_s(\sigma_{m_i})$, $P_s(\sigma_{t_i})$ and $P_s(p_{T_i})$ are described by Gamma functions. They are unchanged from the previous analysis and explained in detail in ref. [6]. Ignoring detector effects, the joint distribution for the decay time t and the transversity angles Ω for the $B_s^0 \rightarrow J/\psi(\mu^+\mu^-)\phi(K^+K^-)$ decay is given by the differential decay rate [22]:

$$\frac{d^4\Gamma}{dt d\Omega} = \sum_{k=1}^{10} \mathcal{O}^{(k)}(t) g^{(k)}(\theta_T, \psi_T, \phi_T),$$

where $\mathcal{O}^{(k)}(t)$ are the time-dependent amplitudes and $g^{(k)}(\theta_T, \psi_T, \phi_T)$ are the angular functions, given in table II. The formulae for the time-dependent amplitudes have the same structure for B_s^0 and \bar{B}_s^0 but with a sign reversal in the terms containing Δm_s . The addition of flavour tagging to the analysis means that these terms no longer cancel, so there are more terms in the fit that contain ϕ_s . In addition to this, the strong phase variable δ_{\perp} becomes accessible and one of the symmetries in the untagged fit is removed. $A_{\perp}(t)$ describes a CP odd final-state configuration while both $A_0(t)$ and $A_{\parallel}(t)$ correspond to CP even final-state configurations. $A_S(t)$ describes the contribution of the CP odd non-resonant $B_s^0 \rightarrow J/\psi K^+K^-$ S -wave state as well as the $B_s^0 \rightarrow J/\psi f_0$ decays. The corresponding amplitudes are given in the last four lines of table II ($k = 7-10$) and follow the convention used in the previous analysis [23]. The likelihood is independent of the K^+K^- mass distribution.

k	$\mathcal{O}^{(k)}(t)$	$g^{(k)}(\theta_T, \psi_T, \phi_T)$
1	$\frac{1}{2} A_0(0) ^2 \left[(1 + \cos \phi_s) e^{-\Gamma_L^{(s)} t} + (1 - \cos \phi_s) e^{-\Gamma_H^{(s)} t} \pm 2e^{-\Gamma_s t} \sin(\Delta m_s t) \sin \phi_s \right]$	$2 \cos^2 \psi_T (1 - \sin^2 \theta_T \cos^2 \phi_T)$
2	$\frac{1}{2} A_{\parallel}(0) ^2 \left[(1 + \cos \phi_s) e^{-\Gamma_L^{(s)} t} + (1 - \cos \phi_s) e^{-\Gamma_H^{(s)} t} \pm 2e^{-\Gamma_s t} \sin(\Delta m_s t) \sin \phi_s \right]$	$\sin^2 \psi_T (1 - \sin^2 \theta_T \sin^2 \phi_T)$
3	$\frac{1}{2} A_{\perp}(0) ^2 \left[(1 - \cos \phi_s) e^{-\Gamma_L^{(s)} t} + (1 + \cos \phi_s) e^{-\Gamma_H^{(s)} t} \mp 2e^{-\Gamma_s t} \sin(\Delta m_s t) \sin \phi_s \right]$	$\sin^2 \psi_T \sin^2 \theta_T$
4	$\frac{1}{2} A_0(0) A_{\parallel}(0) \cos \delta_{\parallel} \left[(1 + \cos \phi_s) e^{-\Gamma_L^{(s)} t} + (1 - \cos \phi_s) e^{-\Gamma_H^{(s)} t} \pm 2e^{-\Gamma_s t} \sin(\Delta m_s t) \sin \phi_s \right]$	$-\frac{1}{\sqrt{2}} \sin 2\psi_T \sin^2 \theta_T \sin 2\phi_T$
5	$ A_{\parallel}(0) A_{\perp}(0) \left[\frac{1}{2}(e^{-\Gamma_L^{(s)} t} - e^{-\Gamma_H^{(s)} t}) \cos(\delta_{\perp} - \delta_{\parallel}) \sin \phi_s \right. \\ \left. \pm e^{-\Gamma_s t} (\sin(\delta_{\perp} - \delta_{\parallel}) \cos(\Delta m_s t) - \cos(\delta_{\perp} - \delta_{\parallel}) \cos \phi_s \sin(\Delta m_s t)) \right]$	$\sin^2 \psi_T \sin 2\theta_T \sin \phi_T$
6	$ A_0(0) A_{\perp}(0) \left[\frac{1}{2}(e^{-\Gamma_L^{(s)} t} - e^{-\Gamma_H^{(s)} t}) \cos \delta_{\perp} \sin \phi_s \right. \\ \left. \pm e^{-\Gamma_s t} (\sin \delta_{\perp} \cos(\Delta m_s t) - \cos \delta_{\perp} \cos \phi_s \sin(\Delta m_s t)) \right]$	$\frac{1}{\sqrt{2}} \sin 2\psi_T \sin 2\theta_T \cos \phi_T$
7	$\frac{1}{2} A_S(0) ^2 \left[(1 - \cos \phi_s) e^{-\Gamma_L^{(s)} t} + (1 + \cos \phi_s) e^{-\Gamma_H^{(s)} t} \mp 2e^{-\Gamma_s t} \sin(\Delta m_s t) \sin \phi_s \right]$	$\frac{2}{3} (1 - \sin^2 \theta_T \cos^2 \phi_T)$
8	$ A_S(0) A_{\parallel}(0) \left[\frac{1}{2}(e^{-\Gamma_L^{(s)} t} - e^{-\Gamma_H^{(s)} t}) \sin(\delta_{\parallel} - \delta_S) \sin \phi_s \right. \\ \left. \pm e^{-\Gamma_s t} (\cos(\delta_{\parallel} - \delta_S) \cos(\Delta m_s t) - \sin(\delta_{\parallel} - \delta_S) \cos \phi_s \sin(\Delta m_s t)) \right]$	$\frac{1}{3} \sqrt{6} \sin \psi_T \sin^2 \theta_T \sin 2\phi_T$
9	$\frac{1}{2} A_S(0) A_{\perp}(0) \sin(\delta_{\perp} - \delta_S) \left[(1 - \cos \phi_s) e^{-\Gamma_L^{(s)} t} + (1 + \cos \phi_s) e^{-\Gamma_H^{(s)} t} \mp 2e^{-\Gamma_s t} \sin(\Delta m_s t) \sin \phi_s \right]$	$\frac{1}{3} \sqrt{6} \sin \psi_T \sin 2\theta_T \cos \phi_T$
10	$ A_0(0) A_S(0) \left[\frac{1}{2}(e^{-\Gamma_H^{(s)} t} - e^{-\Gamma_L^{(s)} t}) \sin \delta_S \sin \phi_s \right. \\ \left. \pm e^{-\Gamma_s t} (\cos \delta_S \cos(\Delta m_s t) + \sin \delta_S \cos \phi_s \sin(\Delta m_s t)) \right]$	$\frac{4}{3} \sqrt{3} \cos \psi_T (1 - \sin^2 \theta_T \cos^2 \phi_T)$

TABLE II. Table showing the ten time-dependent amplitudes, $\mathcal{O}^{(k)}(t)$ and the functions of the transversity angles $g^{(k)}(\theta_T, \psi_T, \phi_T)$. The amplitudes $|A_0(0)|^2$ and $|A_{\parallel}(0)|^2$ are for the CP even components of the $B_s^0 \rightarrow J/\psi \phi$ decay, $|A_{\perp}(0)|^2$ is the CP odd amplitude; they have corresponding strong phases δ_0 , δ_{\parallel} and δ_{\perp} , by convention δ_0 is set to be zero. The S -wave amplitude $|A_S(0)|^2$ gives the fraction of $B_s^0 \rightarrow J/\psi K^+ K^- (f_0)$ and has a related strong phase δ_S . The \pm and \mp terms denote two cases: the upper sign describes the decay of a meson that was initially a B_s^0 , while the lower sign describes the decays of a meson that was initially \bar{B}_s^0 .

The equations are normalized, such that the squares of the amplitudes sum to unity; three of the four amplitudes are fit parameters and $|A_{\perp}(0)|^2$ is determined according to this constraint.

The angles $(\theta_T, \psi_T, \phi_T)$, are defined in the rest frames of the final-state particles. The x -axis is determined by the direction of the ϕ meson in the J/ψ rest frame, and the $K^+ K^-$ system defines the x - y plane, where $p_y(K^+) > 0$. The three angles are defined as follows:

- θ_T , the angle between $\vec{p}(\mu^+)$ and the normal to the x - y plane, in the J/ψ meson rest frame
- ϕ_T , the angle between the x -axis and $\vec{p}_{xy}(\mu^+)$, the projection of the μ^+ momentum in the x - y plane, in the J/ψ meson rest frame
- ψ_T , the angle between $\vec{p}(K^+)$ and $-\vec{p}(J/\psi)$ in the ϕ meson rest frame

The signal PDF, $P_s(\Omega, t, P(B|Q), \sigma_t)$, needs to take into account lifetime resolution, so each time element in table II is smeared with a Gaussian function. This smearing is done numerically on an event-by-event basis where the width of the Gaussian function is the proper decay time uncertainty, measured for each event, multiplied by a scale factor to account for any mis-measurements.

The angular sculpting of the detector and kinematic cuts on the angular distributions are included in the likelihood function through $A(\Omega_i, p_{T_i})$. This is calculated using a 4D binned acceptance method, applying an event-by-event efficiency according to the transversity angles $(\theta_T, \psi_T, \phi_T)$ and the p_T of the candidate. The p_T binning is necessary, because the angular sculpting is influenced by the p_T of the B_s^0 . The acceptance was calculated from the $B_s^0 \rightarrow J/\psi \phi$ MC events. In the likelihood function, the acceptance is treated as an angular sculpting PDF, which is multiplied with the time- and angular-dependent PDF describing the $B_s^0 \rightarrow J/\psi(\mu^+ \mu^-) \phi(K^+ K^-)$ decays. As both the acceptance and time-angular decay PDFs depend on the transversity angles they must be normalized together. This normalization is done numerically during the likelihood fit.

The signal mass function, $P_s(m)$, is modelled using a single Gaussian function smeared with an event-by-event mass resolution. The PDF is normalized over the range $5.15 < m(B_s^0) < 5.65$ GeV.

B. Using tag information in the fit

The tag probability for each B_s^0 candidate is determined from a weighted sum of charged-particle tracks

in a cone, as described in section IV. The tag probability is obtained from this tag charge using the calibrations measured in the $B^\pm \rightarrow J/\psi K^\pm$ data. For the case where there is only one track, the cone charge can only be ± 1 . This leads to a tag probability distribution with continuous and discrete parts (spikes), which are estimated separately. The distributions of tag probabilities for the signal and background are also different and since the background cannot be factorized out, extra PDF terms are included to account for this difference.

To describe the continuous parts, the sidebands are parameterized first. Sidebands are selected according to B_s^0 mass, i.e. $m(B_s^0) < 5.317$ GeV or $m(B_s^0) > 5.417$ GeV. In the fit the same function as for the sidebands is used to describe events in the signal region: background parameters are fixed to the values obtained in sidebands while signal parameters are free in this step. The ratio of background to signal (obtained from simultaneous mass–lifetime fit) is fixed as well. The function describing tagging using combined muons has the form of a fourth-order Chebychev polynomial. A third-order polynomial is used for the segment tagged muons’ tagging algorithm. A fourth-order Chebychev polynomial is also applied for the jet charge tagging algorithm. In all three cases unbinned maximum likelihood fits are used. Results of fits projected on histograms are shown in figure 4.

The spikes have their origin in tagging objects formed from a single track, providing a tag charge of exactly $+1$ or -1 . When a background candidate is formed from a random combination of a J/ψ and a pair of tracks, the positive and negative charges are equally probable. However, some of the background events are formed of partially reconstructed B hadrons, and in these cases tag charges of $+1$ or -1 are not equally probable. For signal events the tag charges are obviously not symmetric. The fractions f_{+1} and f_{-1} of events tagged with charges of $+1$ and -1 are derived separately for signal and background. The remaining $(1 - f_{+1} - f_{-1})$ is the fraction of events in the continuous region. The fractions f_{+1} and f_{-1} are determined using the same B_s^0 mass sidebands and signal regions as in case of continuous parts. Table III summarizes the obtained relative probabilities between tag charges $+1$ and -1 for signal and background events and for all tag methods.

Similarly, the sideband subtraction method is also used to determine, for signal and background events, the relative fraction of each tagging method. The results are summarized in table IV.

If the tag-probability PDFs were ignored in the likelihood fit, equivalent to assuming identical signal and background behaviour, the impact on the fit result would be small, affecting the results by less than 10% of the statistical uncertainty.

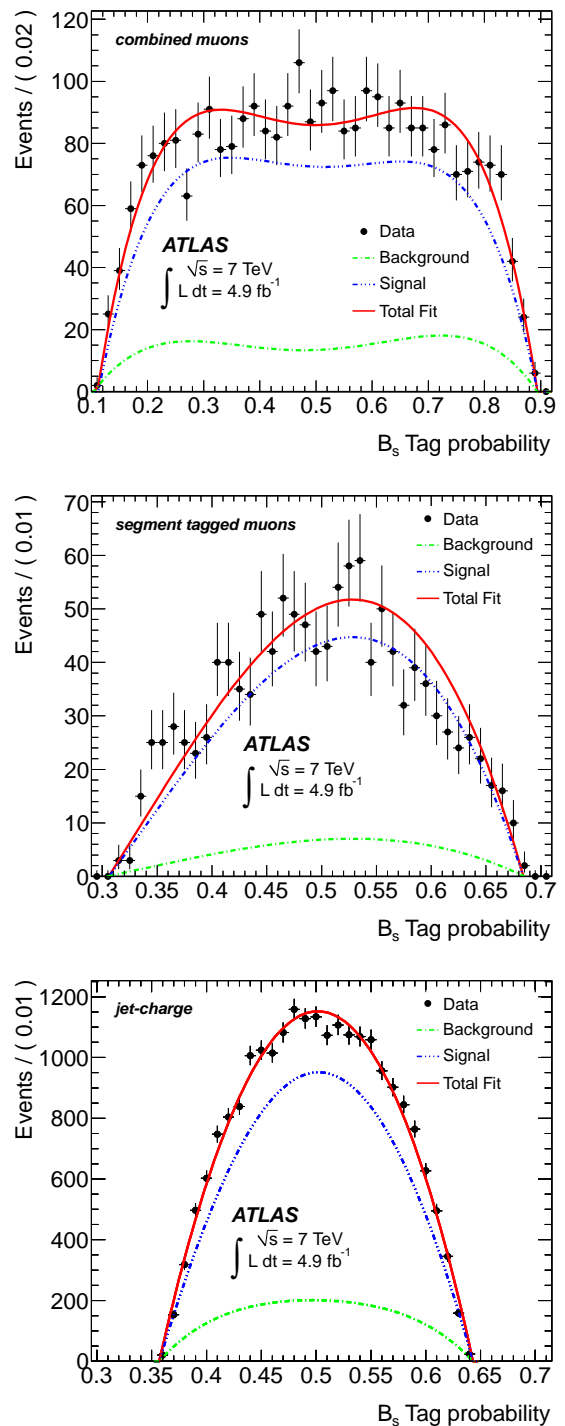


FIG. 4. The B_s^0 -tag probability distribution for the events tagged with combined muons (top), segment tagged muons (middle) and jet charge (bottom). Black dots are data after removing spikes, blue is the fit to the sidebands, green to the signal and red is a sum of both fits.

Tag method	Signal		Background	
	f_{+1}	f_{-1}	f_{+1}	f_{-1}
Combined μ	0.106 ± 0.019	0.187 ± 0.022	0.098 ± 0.006	0.108 ± 0.006
Segment tag μ	0.152 ± 0.043	0.153 ± 0.043	0.098 ± 0.009	0.095 ± 0.008
Jet charge	0.167 ± 0.010	0.164 ± 0.010	0.176 ± 0.003	0.180 ± 0.003

TABLE III. Table summarizing the obtained relative probabilities between tag charges +1 and -1 for signal and background events for the different tagging methods. Only statistical errors are quoted. The asymmetry in the signal combined-muon tagging method has no impact on the results as it affects only 1% of the signal events (in addition to the negligible effect of the tag-probability distributions themselves).

Tag method	Signal	Background
Combined μ	0.0372 ± 0.0023	0.0272 ± 0.0005
Segment tag μ	0.0111 ± 0.0014	0.0121 ± 0.0003
Jet charge	0.277 ± 0.007	0.254 ± 0.002
Untagged	0.675 ± 0.011	0.707 ± 0.003

TABLE IV. Table summarizing the relative population of the tagging methods in the background and signal events. Only statistical errors are quoted.

VI. RESULTS

The full simultaneous maximum likelihood fit contains 25 free parameters. These include the nine physics parameters: $\Delta\Gamma_s$, ϕ_s , Γ_s , $|A_0(0)|^2$, $|A_{\parallel}(0)|^2$, δ_{\parallel} , δ_{\perp} , $|A_S|^2$ and δ_S . The other parameters in the likelihood function are the B_s^0 signal fraction f_s , the parameters describing the $J/\psi\phi$ mass distribution, the parameters describing the B_s^0 meson decay time plus angular distributions of background events, the parameters used to describe the estimated decay time uncertainty distributions for signal and background events, and scale factors between the estimated decay time and mass uncertainties and their true uncertainties.

The number of signal B_s^0 meson candidates extracted from the fits is 22670 ± 150 . The results and correlations for the measured physics parameters of the simultaneous unbinned maximum likelihood fit are given in tables V and VI. Fit projections of the mass, proper decay time and angles are given in figures 5 and 6 respectively.

Parameter	Value	Statistical uncertainty	Systematic uncertainty
ϕ_s [rad]	0.12	0.25	0.05
$\Delta\Gamma_s$ [ps $^{-1}$]	0.053	0.021	0.010
Γ_s [ps $^{-1}$]	0.677	0.007	0.004
$ A_{\parallel}(0) ^2$	0.220	0.008	0.009
$ A_0(0) ^2$	0.529	0.006	0.012
$ A_S(0) ^2$	0.024	0.014	0.028
δ_{\perp}	3.89	0.47	0.11
δ_{\parallel}		[3.04, 3.23]	0.09
$\delta_{\perp} - \delta_S$		[3.02, 3.25]	0.04

TABLE V. Fitted values for the physical parameters with their statistical and systematic uncertainties. For the parameters δ_{\parallel} and $\delta_{\perp} - \delta_S$ a 68% confidence level interval is given. The reason for this is described in section 8.

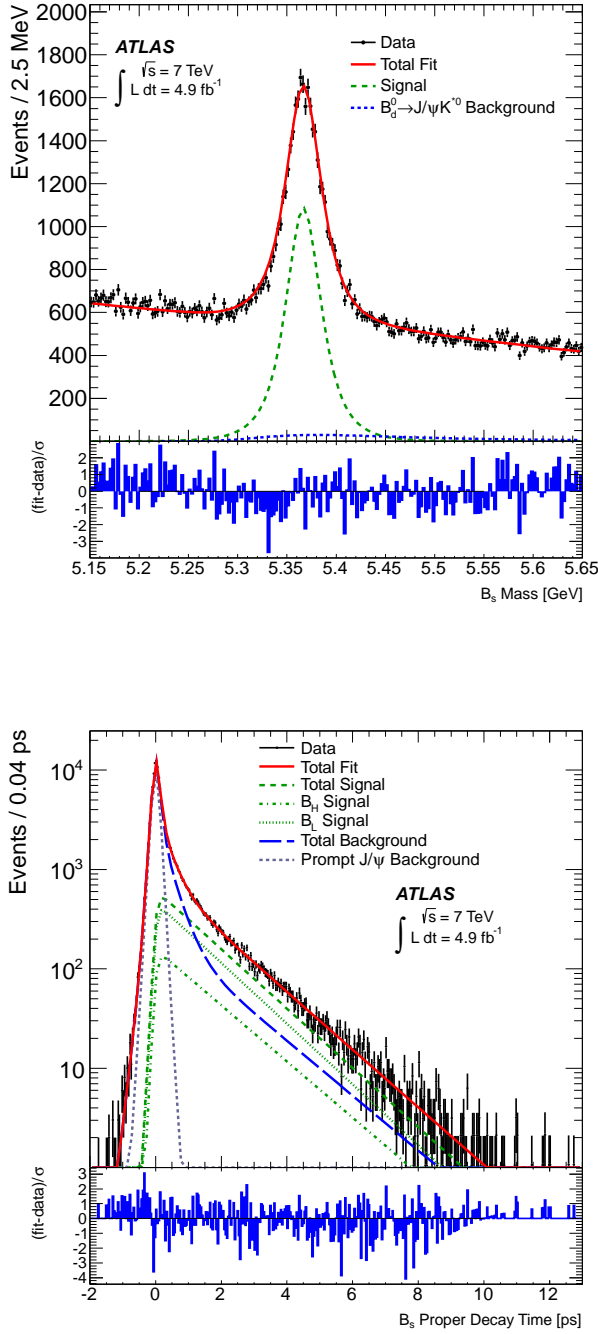


FIG. 5. (Top) Mass fit projection for the $B_s^0 \rightarrow J/\psi\phi$. The red line shows the total fit, the dashed green line shows the signal component while the dotted blue line shows the contribution from $B^0 \rightarrow J/\psi K^{0*}$ events. (Bottom) Proper decay time fit projection for the $B_s^0 \rightarrow J/\psi\phi$. The red line shows the total fit while the green dashed line shows the total signal. The light and heavy components of the signal are shown in green as a dotted and a dash-dotted line, respectively. The total background is shown as a blue dashed line with a grey dotted line showing the prompt J/ψ background. The pull distributions at the bottom show the difference between data and fit value normalized to the data statistical uncertainty.

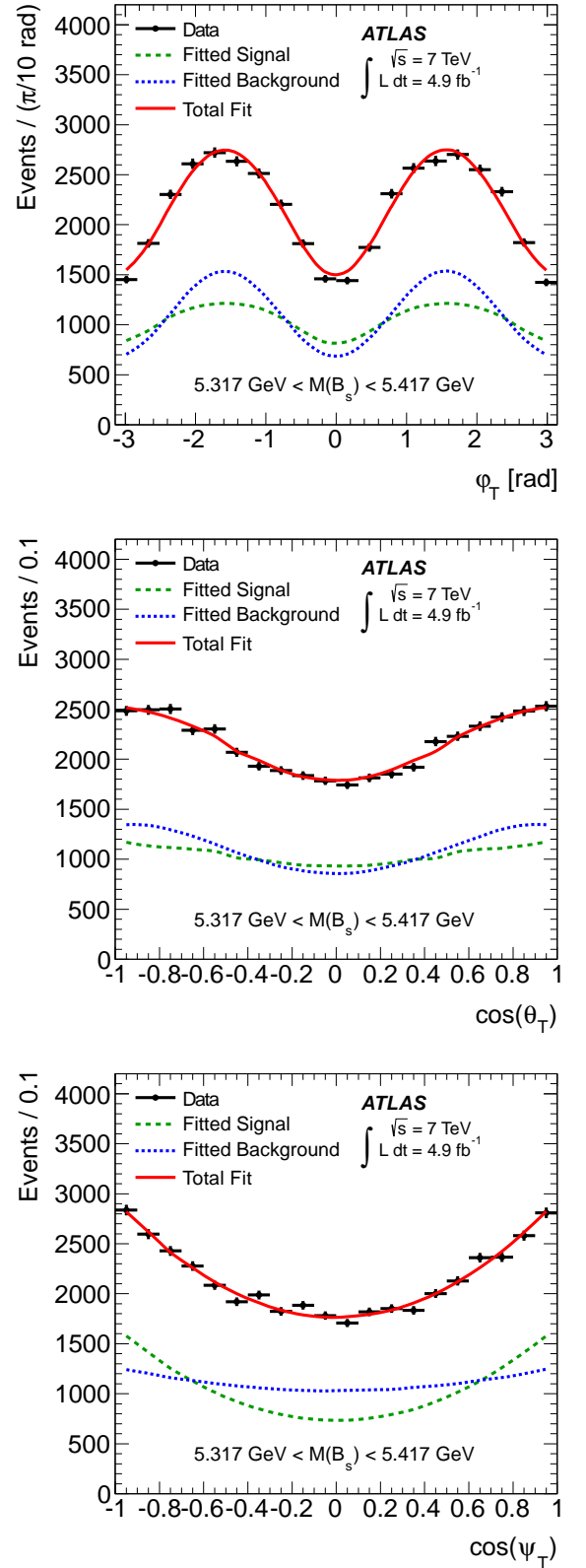


FIG. 6. Fit projections for transversity angles. (Top): ϕ_T , (middle): $\cos\theta_T$, (bottom): $\cos\psi_T$. In all three plots, the red line shows the total fit, the dashed green line shows the signal component and the dotted blue line shows the background contribution.

VII. SYSTEMATIC UNCERTAINTIES

Systematic uncertainties are assigned by considering several effects that are not accounted for in the likelihood fit. These are described below.

- **Inner detector alignment:** Residual mis-alignments of the inner detector affects the impact parameter distribution with respect to the primary vertex. The effect of the residual mis-alignment is estimated using simulated events with and without distorted geometry. For this, the impact parameter distribution with respect to the primary vertex is measured with data as a function of η and ϕ with the maximum deviation from zero being less than $10 \mu\text{m}$. The measurement is used to distort the geometry for simulated events in order to reproduce the impact parameter distribution measured as a function of η and ϕ . The difference between the measurement using simulated events with and without the distorted geometry is used as the systematic uncertainty.
- **Trigger efficiency:** It is observed that the muon trigger biases the transverse impact parameter of muons toward smaller values. To correct for this bias the events are re-weighted according to

$$w = e^{-|t|/(\tau_{\text{sing}}+\epsilon)} / e^{-|t|/\tau_{\text{sing}}},$$

where τ_{sing} is a single B_s^0 lifetime measured before the correction, using an unbinned mass–lifetime maximum likelihood fit. The value of the parameter ϵ and its uncertainty are described in [6]. The systematic uncertainty is calculated by varying the value of ϵ by its uncertainty and rerunning the fit.

- **B^0 contribution:** Contaminations from $B^0 \rightarrow J/\psi K^{0*}$ and $B^0 \rightarrow J/\psi K\pi$ events mis-reconstructed as $B_s^0 \rightarrow J/\psi\phi$ are accounted for in the default fit. The fractions of $B^0 \rightarrow J/\psi K^{0*}$ and $B^0 \rightarrow J/\psi K\pi$ events in the default fit are $(6.5 + / - 2.4)\%$ and $(4.5 + / - 2.8)\%$ respectively. They were determined in MC simulation and using branching fractions from ref. [17]. To estimate the systematic uncertainty arising from the precision of the fraction estimates, the data are fitted with these fractions increased and decreased by 1σ . The largest shifts in the fitted values from the default case are taken as the systematic uncertainty for each parameter of interest.
- **Tagging:** For the uncertainties in the fit parameters due to uncertainty in the tagging, the statistical and systematic components are separated. The statistical uncertainty is due to the sample size of $B^\pm \rightarrow J/\psi K^\pm$ decays available and is included in the overall statistical error. The systematic uncertainty arises from the precision of the tagging calibration and is estimated by varying the model parameterizing the probability distribution, $P(B|Q)$,

as a function of tag charge. The default model is a linear function. For the combined-muon cone-charge tag and the segment tagged muons the alternative fit function is a third-order polynomial. For the jet-charge tag with no muons, a third- and a fifth-order polynomial are used. The B_s^0 fit was repeated using the alternative models and the largest difference was assigned as the systematic uncertainty.

- **Angular acceptance method:** The angular acceptance is calculated from a binned fit to Monte Carlo data. A separate set of Monte Carlo signal events were generated and fully simulated. Background was generated using pseudo-experiments as described below. There is sufficient data to perform 166 fits. The systematic uncertainty is calculated using the bias of the pull distribution multiplied by the statistical uncertainty of each parameter. In order to estimate the size of the systematic uncertainty introduced from the choice of binning, different acceptance functions are calculated using different bin widths and central values. These effects are found to be negligible.
- **Signal and background mass model, resolution model, background lifetime and background angles model:** In order to estimate the size of systematic uncertainties caused by the assumptions made in the fit model, variations of the model are tested in pseudo-experiments. A set of 2400 pseudo-experiments is generated for each variation considered, and fitted with the default model. The systematic error quoted for each effect is the difference between the mean shift of the fitted value of each parameter from its input value for the pseudo-experiments with the systematic alteration included. The variations are: two different scale factors are used to generate the signal mass; the background mass is generated from an exponential function; two different scale factors are used to generate the lifetime uncertainty; the background lifetimes are generated by sampling data from the mass sidebands; pseudo-experiments are generated with background angles taken from histograms from sideband data and are fitted with the default fit model to assess the systematic uncertainty to the parameterization of the background angles in the fit.
- **Default fit model:** The systematic uncertainty of the default fit model is calculated using the bias of the pull distribution of 2400 pseudo-experiments, multiplied by the statistical uncertainty of each parameter.

The systematic uncertainties are provided in table VII. For each variable, the total systematic error is obtained by adding in quadrature the different contributions.

	ϕ_s	$\Delta\Gamma$	Γ_s	$ A_{ }(0) ^2$	$ A_0(0) ^2$	$ A_S(0) ^2$	$\delta_{ }$	δ_{\perp}	$\delta_{\perp} - \delta_S$
ϕ_s	1.000	0.107	0.026	0.010	0.002	0.029	0.021	-0.043	-0.003
$\Delta\Gamma$		1.000	-0.617	0.105	0.103	0.069	0.006	-0.017	0.001
Γ_s			1.000	-0.093	-0.063	0.034	-0.003	0.001	-0.009
$ A_{ }(0) ^2$				1.000	-0.316	0.077	0.008	0.005	-0.010
$ A_0(0) ^2$					1.000	0.283	-0.003	-0.016	-0.025
$ A_S(0) ^2$						1.000	-0.011	-0.054	-0.098
$\delta_{ }$							1.000	0.038	0.007
δ_{\perp}								1.000	0.081
$\delta_{\perp} - \delta_S$									1.000

TABLE VI. Correlations between the physics parameters.

	ϕ_s [rad]	$\Delta\Gamma_s$ [ps ⁻¹]	Γ_s [ps ⁻¹]	$ A_{ }(0) ^2$	$ A_0(0) ^2$	$ A_S(0) ^2$	δ_{\perp} [rad]	$\delta_{ }$ [rad]	$\delta_{\perp} - \delta_S$ [rad]
ID alignment	$<10^{-2}$	$<10^{-3}$	$<10^{-3}$	$<10^{-3}$	$<10^{-3}$	-	$<10^{-2}$	$<10^{-2}$	-
Trigger efficiency	$<10^{-2}$	$<10^{-3}$	0.002	$<10^{-3}$	$<10^{-3}$	$<10^{-3}$	$<10^{-2}$	$<10^{-2}$	$<10^{-2}$
B^0 contribution	0.03	0.001	$<10^{-3}$	$<10^{-3}$	0.005	0.001	0.02	$<10^{-2}$	$<10^{-2}$
Tagging	0.03	$<10^{-3}$	$<10^{-3}$	$<10^{-3}$	$<10^{-3}$	$<10^{-3}$	0.04	$<10^{-2}$	$<10^{-2}$
Acceptance	0.02	0.004	0.002	0.002	0.004	-	-	$<10^{-2}$	-
Models:									
Default fit	$<10^{-2}$	0.003	$<10^{-3}$	0.001	0.001	0.006	0.07	0.01	0.01
Signal mass	$<10^{-2}$	0.001	$<10^{-3}$	$<10^{-3}$	0.001	$<10^{-3}$	0.03	0.04	0.01
Background mass	$<10^{-2}$	0.001	0.001	$<10^{-3}$	$<10^{-3}$	0.002	0.06	0.02	0.02
Resolution	0.02	$<10^{-3}$	0.001	0.001	$<10^{-3}$	0.002	0.04	0.02	0.01
Background time	0.01	0.001	$<10^{-3}$	0.001	$<10^{-3}$	0.002	0.01	0.02	0.02
Background angles	0.02	0.008	0.002	0.008	0.009	0.027	0.06	0.07	0.03
Total	0.05	0.010	0.004	0.009	0.012	0.028	0.11	0.09	0.04

TABLE VII. Summary of systematic uncertainties assigned to the physics parameters.

VIII. DISCUSSION

The PDF describing the $B_s^0 \rightarrow J/\psi\phi$ decay is invariant under the following simultaneous transformations:

$$\{\phi_s, \Delta\Gamma_s, \delta_{\perp}, \delta_{||}\} \rightarrow \{\pi - \phi_s, -\Delta\Gamma_s, \pi - \delta_{\perp}, 2\pi - \delta_{||}\}$$

$\Delta\Gamma_s$ has been determined to be positive [24]. Therefore there is a unique solution and only the case $\Delta\Gamma_s > 0$ is considered. Uncertainties on individual parameters were studied in detail in likelihood scans. Figure 7 shows the 1D likelihood scans for ϕ_s and $\Delta\Gamma_s$. Figure 8 shows the likelihood contours in the $\phi_s - \Delta\Gamma_s$ plane.

The behaviour of the amplitudes around their fitted values is Gaussian, however the strong phases are more complicated. Figure 9 shows the 1D likelihood scans for the three measured strong phases.

The likelihood behaviour of δ_{\perp} appears Gaussian and therefore it is reasonable to quote $\delta_{\perp} = 3.89 \pm 0.47(stat)$ rad. For $\delta_{\perp} - \delta_S$ the scan shows a minimum close to π ; however, it is insensitive over the rest of the scan at

the level of 2.1σ . Therefore the measured value of the difference $\delta_{\perp} - \delta_S$ is only given as 1σ confidence interval [3.02, 3.25] rad. For the strong phase $\delta_{||}$ the central fit value is close to π (3.14 ± 0.10) and the 1D likelihood scan shows normal Gaussian behaviour around this minimum. However, the systematic pull plot based on 2400 pseudo-experiments fits reveals a double-Gaussian shape with 68% of the results included in the interval [2.92, 3.35] rad and so we quote the result in the form of a 68% C.L. interval $\delta_{||} \in [2.92, 3.35]$ rad (statistical only).

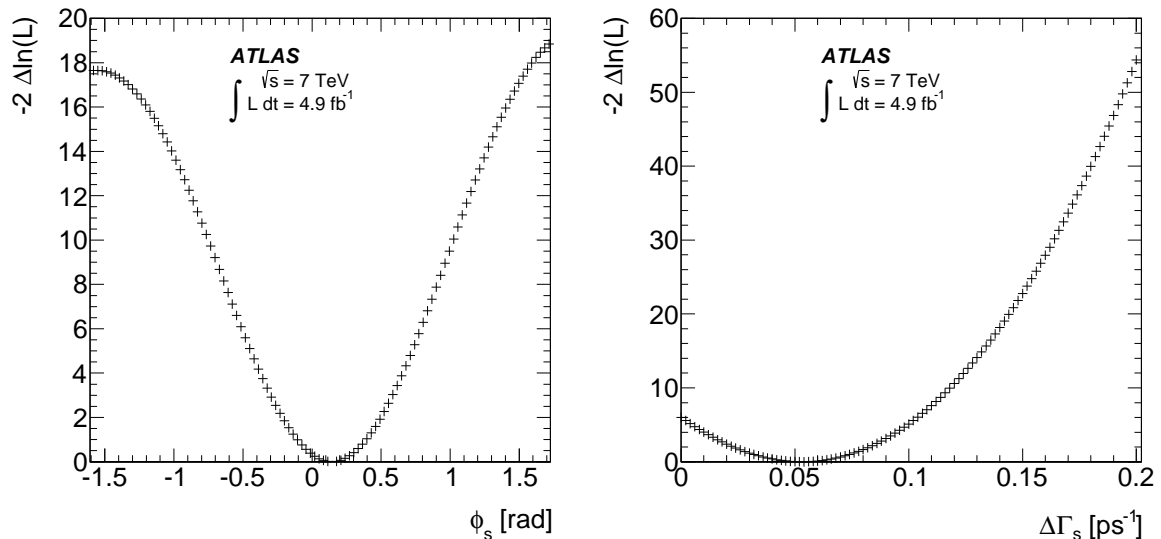


FIG. 7. 1D likelihood scans for ϕ_s (left) and $\Delta\Gamma_s$ (right).

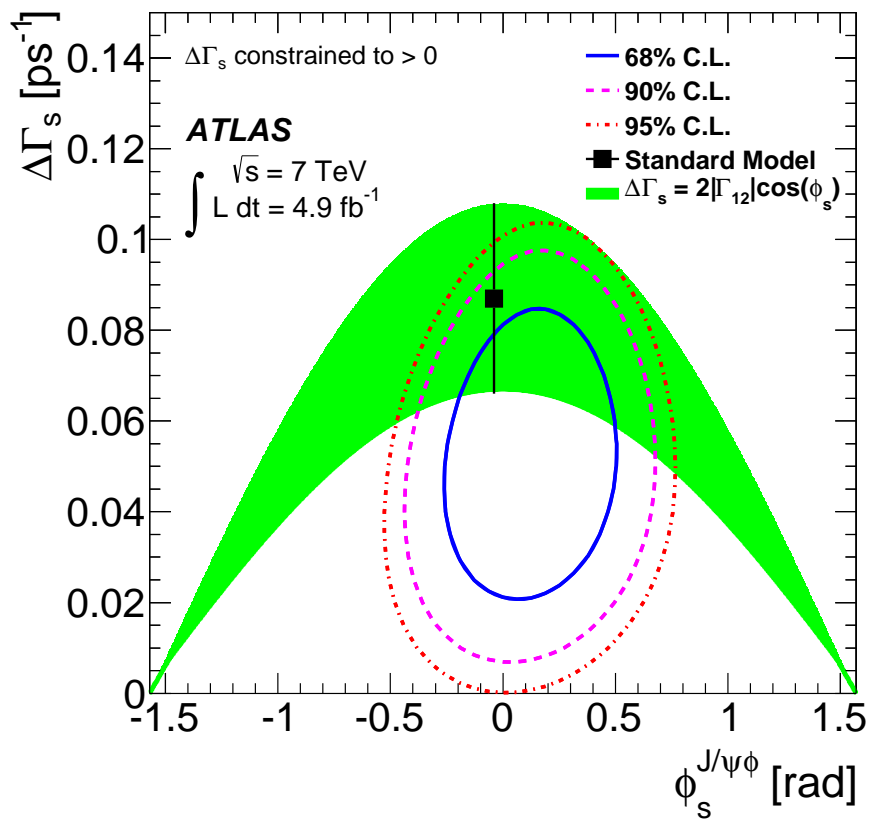


FIG. 8. Likelihood contours in the $\phi_s - \Delta\Gamma_s$ plane. The blue line shows the 68% likelihood contour, the dashed pink line shows the 90% likelihood contour and the red dotted line shows the 95% likelihood contour (statistical errors only). The green band is the theoretical prediction of mixing-induced CP violation.

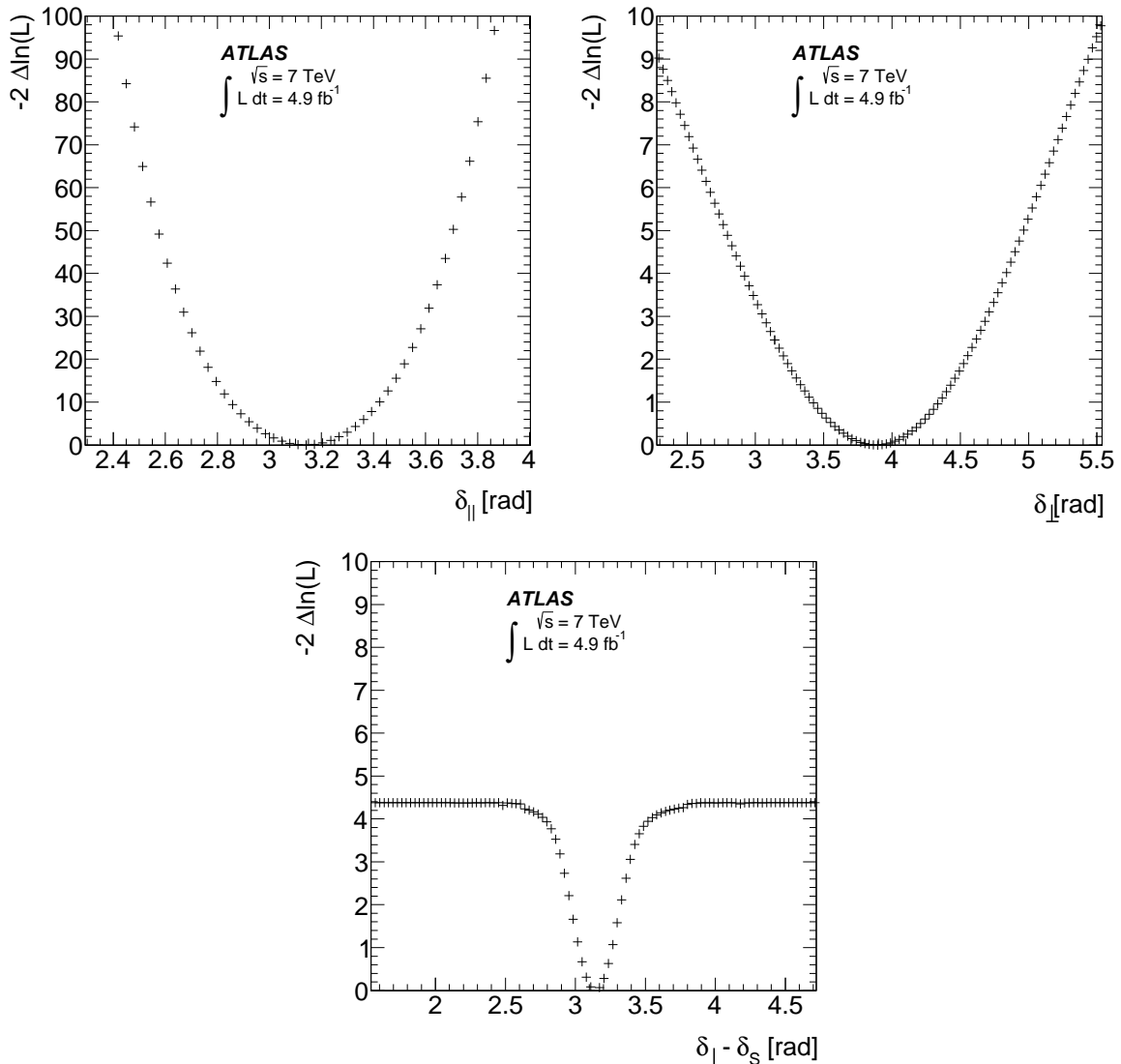


FIG. 9. 1D likelihood scans for δ_{\parallel} (top left), δ_{\perp} (top right) and $\delta_{\perp} - \delta_S$ (bottom).

IX. CONCLUSION

A measurement of time-dependent CP asymmetry parameters in $B_s^0 \rightarrow J/\psi(\mu^+\mu^-)\phi(K^+K^-)$ decays from a 4.9fb^{-1} data sample of pp collisions collected with the ATLAS detector during the 2011 $\sqrt{s} = 7$ TeV LHC run is presented. Several parameters describing the B_s^0 meson system are measured. These include the mean B_s^0 lifetime $1/\Gamma_s$, the decay width difference $\Delta\Gamma_s$ between the heavy and light mass eigenstates, and the transversity amplitudes $|A_0(0)|$ and $|A_{\parallel}(0)|$. Each of these is consistent with its respective world average. Likelihood contours in the $\phi_s - \Delta\Gamma_s$ plane are also provided. The fraction $|A_S(0)|^2$, the signal contribution from $B_s^0 \rightarrow J/\psi K^+K^-$ and $B_s^0 \rightarrow J/\psi f_0$ decays, is measured to be consistent with zero, at 0.024 ± 0.014 (stat.) ± 0.028 (syst.).

The results are:

$$\begin{aligned}
 \phi_s &= 0.12 \pm 0.25 \text{ (stat.)} \pm 0.05 \text{ (syst.) rad} \\
 \Delta\Gamma_s &= 0.053 \pm 0.021 \text{ (stat.)} \pm 0.010 \text{ (syst.) ps}^{-1} \\
 \Gamma_s &= 0.677 \pm 0.007 \text{ (stat.)} \pm 0.004 \text{ (syst.) ps}^{-1} \\
 |A_{\parallel}(0)|^2 &= 0.220 \pm 0.008 \text{ (stat.)} \pm 0.009 \text{ (syst.)} \\
 |A_0(0)|^2 &= 0.529 \pm 0.006 \text{ (stat.)} \pm 0.012 \text{ (syst.)} \\
 \delta_{\perp} &= 3.89 \pm 0.47 \text{ (stat.)} \pm 0.11 \text{ (syst.) rad}
 \end{aligned}$$

The values are consistent with those obtained in our untagged analysis [6] and significantly reduce the overall uncertainty on ϕ_s . These results are consistent with the values predicted in the Standard Model.

ACKNOWLEDGMENTS

We thank CERN for the very successful operation of the LHC, as well as the support staff from our institutions without whom ATLAS could not be operated efficiently.

We acknowledge the support of ANPCyT, Argentina; YerPhI, Armenia; ARC, Australia; BMWF and FWF, Austria; ANAS, Azerbaijan; SSTC, Belarus; CNPq and FAPESP, Brazil; NSERC, NRC and CFI, Canada; CERN; CONICYT, Chile; CAS, MOST and NSFC, China; COLCIENCIAS, Colombia; MSMT CR, MPO CR and VSC CR, Czech Republic; DNRF, DNSRC and Lundbeck Foundation, Denmark; EPLANET, ERC and NSRF, European Union; IN2P3-CNRS, CEA-DSM/IRFU, France; GNSF, Georgia; BMBF, DFG, HGF, MPG and AvH Foundation, Germany; GSRT and NSRF, Greece; ISF, MINERVA, GIF, I-CORE and Benoziyo Center, Israel; INFN, Italy; MEXT and JSPS,

Japan; CNRST, Morocco; FOM and NWO, Netherlands; BRF and RCN, Norway; MNiSW and NCN, Poland; GRICES and FCT, Portugal; MNE/IFA, Romania; MES of Russia and ROSATOM, Russian Federation; JINR; MSTD, Serbia; MSSR, Slovakia; ARRS and MIZŠ, Slovenia; DST/NRF, South Africa; MINECO, Spain; SRC and Wallenberg Foundation, Sweden; SER, SNSF and Cantons of Bern and Geneva, Switzerland; NSC, Taiwan; TAEK, Turkey; STFC, the Royal Society and Leverhulme Trust, United Kingdom; DOE and NSF, United States of America.

The crucial computing support from all WLCG partners is acknowledged gratefully, in particular from CERN and the ATLAS Tier-1 facilities at TRIUMF (Canada), NDGF (Denmark, Norway, Sweden), CC-IN2P3 (France), KIT/GridKA (Germany), INFN-CNAF (Italy), NL-T1 (Netherlands), PIC (Spain), ASGC (Taiwan), RAL (UK) and BNL (USA) and in the Tier-2 facilities worldwide.

-
- [1] UTfit Collaboration, M. Bona et al., *Phys. Rev. Lett.* **97** (2006) 151803, [arXiv:hep-ph/0605213](#) [[hep-ph](#)].
- [2] CDF Collaboration, A. Abulencia et al., *Phys. Rev. Lett.* **97** (2006) 242003, [arXiv:hep-ex/0609040](#) [[hep-ex](#)].
- [3] LHCb Collaboration, R. Aaij et al., *Phys. Lett. B* **709** (2012) 177–184, [arXiv:1112.4311](#) [[hep-ex](#)].
- [4] A. Lenz and U. Nierste, [arXiv:1102.4274](#) [[hep-ph](#)].
- [5] A. Lenz and U. Nierste, *JHEP* **06** (2007) 072, [arXiv:hep-ph/0612167](#) [[hep-ph](#)].
- [6] ATLAS Collaboration, *JHEP* **12** (2012) 072, [arXiv:1208.0572](#) [[hep-ex](#)].
- [7] D0 Collaboration, V. M. Abazov et al., *Phys. Rev. D* **85** (2012) 032006, [arXiv:1109.3166](#) [[hep-ex](#)].
- [8] CDF Collaboration, T. Aaltonen et al., *Phys. Rev. Lett.* **109** (2012) 171802, [arXiv:1208.2967](#) [[hep-ex](#)].
- [9] LHCb Collaboration, R. Aaij et al., *Phys. Rev. D* **87** (2013) 112010, [arXiv:1304.2600](#) [[hep-ex](#)].
- [10] ATLAS Collaboration, *JINST* **3** (2008) S08003.
- [11] ATLAS uses a right-handed coordinate system with its origin at the nominal interaction point (IP) in the centre of the detector and the z -axis along the beam pipe. The x -axis points from the IP to the centre of the LHC ring, and the y -axis points upward. Cylindrical coordinates (r, ϕ) are used in the transverse plane, ϕ being the azimuthal angle around the beam pipe. The pseudorapidity is defined in terms of the polar angle θ as $\eta = -\ln \tan(\theta/2)$.
- [12] T. Sjostrand, S. Mrenna, and P. Z. Skands, *JHEP* **05** (2006) 026, [arXiv:hep-ph/0603175](#) [[hep-ph](#)].
- [13] ATLAS Collaboration, ATL-PHYS-PUB-2011-009. <http://cds.cern.ch/record/1363300>.
- [14] ATLAS Collaboration, *Eur. Phys. J. C* **70** (2010) 823–874, [arXiv:1005.4568](#) [[physics.ins-det](#)].
- [15] GEANT4 Collaboration, S. Agostinelli et al., *Nucl. Instrum. Meth. A* **506** (2003) 250–303.
- [16] ATLAS Collaboration, *Nucl. Phys. B* **850** (2011) 387–444, [arXiv:1104.3038](#) [[hep-ex](#)].
- [17] Particle Data Group Collaboration, J. Beringer et al., *Phys. Rev. D* **86** (2012) 010001. (and 2013 partial update for the 2014 edition).
- [18] R. Field and R. Feynman, *Nucl. Phys. B* **136** (1978) 1–76.
- [19] $\Delta R^2 = \Delta\phi^2 + \Delta\eta^2$, where $\Delta\phi$ and $\Delta\eta$ are the differences between the measured ϕ and η of the tracks respectively.
- [20] ATLAS Collaboration, ATLAS-CONF-2011-102. <http://cds.cern.ch/record/1369219>.
- [21] ATLAS Collaboration, [arXiv:0901.0512](#) [[hep-ex](#)].
- [22] A. S. Dighe, I. Dunietz, and R. Fleischer, *Eur. Phys. J. C* **6** (1999) 647–662, [arXiv:hep-ph/9804253](#) [[hep-ph](#)].
- [23] LHCb Collaboration, R. Aaij et al., *Phys. Rev. Lett.* **108** (2012) 101803, [arXiv:1112.3183](#) [[hep-ex](#)].
- [24] LHCb Collaboration, R. Aaij et al., *Phys. Rev. Lett.* **108** (2012) 241801, [arXiv:1202.4717](#) [[hep-ex](#)].

The ATLAS Collaboration

G. Aad⁸⁴, T. Abajyan²¹, B. Abbott¹¹², J. Abdallah¹⁵², S. Abdel Khalek¹¹⁶, O. Abdinov¹¹, R. Aben¹⁰⁶, B. Abi¹¹³, M. Abolins⁸⁹, O.S. AbouZeid¹⁵⁹, H. Abramowicz¹⁵⁴, H. Abreu¹³⁷, Y. Abulaiti^{147a,147b}, B.S. Acharya^{165a,165b,a}, L. Adamczyk^{38a}, D.L. Adams²⁵, T.N. Addy⁵⁶, J. Adelman¹⁷⁷, S. Adomeit⁹⁹, T. Adye¹³⁰, T. Agatonovic-Jovin^{13b}, J.A. Aguilar-Saavedra^{125f,125a}, M. Agustoni¹⁷, S.P. Ahlen²², A. Ahmad¹⁴⁹, F. Ahmadov^{64,b}, G. Aielli^{134a,134b}, T.P.A. Åkesson⁸⁰, G. Akimoto¹⁵⁶, A.V. Akimov⁹⁵, J. Albert¹⁷⁰, S. Albrand⁵⁵, M.J. Alconada Verzini⁷⁰, M. Aleksa³⁰, I.N. Aleksandrov⁶⁴, C. Alexa^{26a}, G. Alexander¹⁵⁴, G. Alexandre⁴⁹, T. Alexopoulos¹⁰, M. Alhroob^{165a,165c}, G. Alimonti^{90a}, L. Alio⁸⁴, J. Alison³¹, B.M.M. Allbrooke¹⁸, L.J. Allison⁷¹, P.P. Allport⁷³, S.E. Allwood-Spiers⁵³, J. Almond⁸³, A. Aloisio^{103a,103b}, R. Alon¹⁷³, A. Alonso³⁶, F. Alonso⁷⁰, C. Alpigiani⁷⁵, A. Altheimer³⁵, B. Alvarez Gonzalez⁸⁹, M.G. Alviggi^{103a,103b}, K. Amako⁶⁵, Y. Amaral Coutinho^{24a}, C. Amelung²³, D. Amidei⁸⁸, V.V. Ammosov^{129,*}, S.P. Amor Dos Santos^{125a,125c}, A. Amorim^{125a,125b}, S. Amoroso⁴⁸, N. Amram¹⁵⁴, G. Amundsen²³, C. Anastopoulos¹⁴⁰, L.S. Ancu¹⁷, N. Andari³⁰, T. Andeen³⁵, C.F. Anders^{58b}, G. Anders³⁰, K.J. Anderson³¹, A. Andreazza^{90a,90b}, V. Andrei^{58a}, X.S. Anduaga⁷⁰, S. Angelidakis⁹, P. Anger⁴⁴, A. Angerami³⁵, F. Anghinolfi³⁰, A.V. Anisenkov¹⁰⁸, N. Anjos^{125a}, A. Annovi⁴⁷, A. Antonaki⁹, M. Antonelli⁴⁷, A. Antonov⁹⁷, J. Antos^{145b}, F. Anulli^{133a}, M. Aoki⁶⁵, L. Aperio Bella¹⁸, R. Apolle^{119,c}, G. Arabidze⁸⁹, I. Aracena¹⁴⁴, Y. Arai⁶⁵, J.P. Araque^{125a}, A.T.H. Arce⁴⁵, J-F. Arguin⁹⁴, S. Argyropoulos⁴², M. Arik^{19a}, A.J. Armbruster³⁰, O. Arnaez⁸², V. Arnal⁸¹, O. Arslan²¹, A. Artamonov⁹⁶, G. Artoni²³, S. Asai¹⁵⁶, N. Asbah⁹⁴, A. Ashkenazi¹⁵⁴, S. Ask²⁸, B. Åsman^{147a,147b}, L. Asquith⁶, K. Assamagan²⁵, R. Astalos^{145a}, M. Atkinson¹⁶⁶, N.B. Atlay¹⁴², B. Auerbach⁶, E. Auge¹¹⁶, K. Augsten¹²⁷, M. Aurousseau^{146b}, G. Avolio³⁰, G. Azuelos^{94,d}, Y. Azuma¹⁵⁶, M.A. Baak³⁰, C. Bacci^{135a,135b}, A.M. Bach¹⁵, H. Bachacou¹³⁷, K. Bachas¹⁵⁵, M. Backes³⁰, M. Backhaus³⁰, J. Backus Mayes¹⁴⁴, E. Badescu^{26a}, P. Bagiacchi^{133a,133b}, P. Bagnaia^{133a,133b}, Y. Bai^{33a}, D.C. Bailey¹⁵⁹, T. Bain³⁵, J.T. Baines¹³⁰, O.K. Baker¹⁷⁷, S. Baker⁷⁷, P. Balek¹²⁸, F. Balli¹³⁷, E. Banas³⁹, Sw. Banerjee¹⁷⁴, D. Banfi³⁰, A. Bangert¹⁵¹, A.A.E. Bannoura¹⁷⁶, V. Bansal¹⁷⁰, H.S. Bansil¹⁸, L. Barak¹⁷³, S.P. Baranov⁹⁵, T. Barber⁴⁸, E.L. Barberio⁸⁷, D. Barberis^{50a,50b}, M. Barbero⁸⁴, T. Barillari¹⁰⁰, M. Barisonzi¹⁷⁶, T. Barklow¹⁴⁴, N. Barlow²⁸, B.M. Barnett¹³⁰, R.M. Barnett¹⁵, Z. Barnovska⁵, A. Baroncelli^{135a}, G. Barone⁴⁹, A.J. Barr¹¹⁹, F. Barreiro⁸¹, J. Barreiro Guimarães da Costa⁵⁷, R. Bartoldus¹⁴⁴, A.E. Barton⁷¹, P. Bartos^{145a}, V. Bartsch¹⁵⁰, A. Bassalat¹¹⁶, A. Basye¹⁶⁶, R.L. Bates⁵³, L. Batkova^{145a}, J.R. Batley²⁸, M. Battistin³⁰, F. Bauer¹³⁷, H.S. Bawa^{144,e}, T. Beau⁷⁹, P.H. Beauchemin¹⁶², R. Beccherle^{123a,123b}, P. Bechtel²¹, H.P. Beck¹⁷, K. Becker¹⁷⁶, S. Becker⁹⁹, M. Beckingham¹³⁹, C. Becot¹¹⁶, A.J. Beddall^{19c}, A. Beddall^{19c}, S. Bedikian¹⁷⁷, V.A. Bednyakov⁶⁴, C.P. Bee¹⁴⁹, L.J. Beemster¹⁰⁶, T.A. Beermann¹⁷⁶, M. Begel²⁵, K. Behr¹¹⁹, C. Belanger-Champagne⁸⁶, P.J. Bell⁴⁹, W.H. Bell⁴⁹, G. Bella¹⁵⁴, L. Bellagamba^{20a}, A. Bellerive²⁹, M. Bellomo⁸⁵, A. Belloni⁵⁷, O.L. Beloborodova^{108,f}, K. Belotskiy⁹⁷, O. Beltramello³⁰, O. Benary¹⁵⁴, D. Benchekroun^{136a}, K. Bendtz^{147a,147b}, N. Benekos¹⁶⁶, Y. Benhammou¹⁵⁴, E. Benhar Nocchioli⁴⁹, J.A. Benitez Garcia^{160b}, D.P. Benjamin⁴⁵, J.R. Bensinger²³, K. Benslama¹³¹, S. Bentvelsen¹⁰⁶, D. Berge¹⁰⁶, E. Bergeaas Kuutmann¹⁶, N. Berger⁵, F. Berghaus¹⁷⁰, E. Berglund¹⁰⁶, J. Beringer¹⁵, C. Bernard²², P. Bernat⁷⁷, C. Bernius⁷⁸, F.U. Bernlochner¹⁷⁰, T. Berry⁷⁶, P. Berta¹²⁸, C. Bertella⁸⁴, F. Bertolucci^{123a,123b}, M.I. Besana^{90a}, G.J. Besjes¹⁰⁵, O. Bessidskaia^{147a,147b}, N. Besson¹³⁷, C. Betancourt⁴⁸, S. Bethke¹⁰⁰, W. Bhimji⁴⁶, R.M. Bianchi¹²⁴, L. Bianchini²³, M. Bianco³⁰, O. Biebel⁹⁹, S.P. Bieniek⁷⁷, K. Bierwagen⁵⁴, J. Biesiada¹⁵, M. Biglietti^{135a}, J. Bilbao De Mendizabal⁴⁹, H. Bilokon⁴⁷, M. Bindi⁵⁴, S. Binet¹¹⁶, A. Bingul^{19c}, C. Bini^{133a,133b}, C.W. Black¹⁵¹, J.E. Black¹⁴⁴, K.M. Black²², D. Blackburn¹³⁹, R.E. Blair⁶, J.-B. Blanchard¹³⁷, T. Blazek^{145a}, I. Bloch⁴², C. Blocker²³, W. Blum^{82,*}, U. Blumenschein⁵⁴, G.J. Bobbink¹⁰⁶, V.S. Bobrovnikov¹⁰⁸, S.S. Bocchetta⁸⁰, A. Bocchi⁴⁵, C.R. Boddy¹¹⁹, M. Boehler⁴⁸, J. Boek¹⁷⁶, T.T. Boek¹⁷⁶, J.A. Bogaerts³⁰, A.G. Bogdanchikov¹⁰⁸, A. Bogouch^{91,*}, C. Bohm^{147a}, J. Bohm¹²⁶, V. Boisvert⁷⁶, T. Bold^{38a}, V. Boldea^{26a}, A.S. Boldyrev⁹⁸, N.M. Bolnet¹³⁷, M. Bomben⁷⁹, M. Bona⁷⁵, M. Boonekamp¹³⁷, A. Borisov¹²⁹, G. Borissov⁷¹, M. Borri⁸³, S. Borroni⁴², J. Bortfeldt⁹⁹, V. Bortolotto^{135a,135b}, K. Bos¹⁰⁶, D. Boscherini^{20a}, M. Bosman¹², H. Boterenbrood¹⁰⁶, J. Boudreau¹²⁴, J. Bouffard², E.V. Bouhova-Thacker⁷¹, D. Boumediene³⁴, C. Bourdarios¹¹⁶, N. Bousson¹¹³, S. Boutouil^{136d}, A. Boveia³¹, J. Boyd³⁰, I.R. Boyko⁶⁴, I. Bozovic-Jelisavcic^{13b}, J. Bracinik¹⁸, P. Branchini^{135a}, A. Brandt⁸, G. Brandt¹⁵, O. Brandt^{58a}, U. Bratzler¹⁵⁷, B. Brau⁸⁵, J.E. Brau¹¹⁵, H.M. Braun^{176,*}, S.F. Brazzale^{165a,165c}, B. Brelier¹⁵⁹, K. Brendlinger¹²¹, A.J. Brennan⁸⁷, R. Brenner¹⁶⁷, S. Bressler¹⁷³, K. Bristow^{146c}, T.M. Bristow⁴⁶, D. Britton⁵³, F.M. Brochu²⁸, I. Brock²¹, R. Brock⁸⁹, C. Bromberg⁸⁹, J. Bronner¹⁰⁰, G. Brooijmans³⁵, T. Brooks⁷⁶, W.K. Brooks^{32b}, J. Brosamer¹⁵, E. Brost¹¹⁵, G. Brown⁸³, J. Brown⁵⁵, P.A. Bruckman de Renstrom³⁹, D. Bruncko^{145b}, R. Bruneliere⁴⁸, S. Brunet⁶⁰, A. Bruni^{20a}, G. Bruni^{20a}, M. Bruschi^{20a}, L. Bryngemark⁸⁰, T. Buanes¹⁴, Q. Buat¹⁴³, F. Bucci⁴⁹, P. Buchholz¹⁴², R.M. Buckingham¹¹⁹, A.G. Buckley⁵³, S.I. Buda^{26a}, I.A. Budagov⁶⁴, F. Buehrer⁴⁸, L. Bugge¹¹⁸, M.K. Bugge¹¹⁸, O. Bulekov⁹⁷, A.C. Bundock⁷³, H. Burckhart³⁰, S. Burdin⁷³, B. Burghgrave¹⁰⁷, S. Burke¹³⁰, I. Burmeister⁴³, E. Busato³⁴, V. Büscher⁸², P. Bussey⁵³, C.P. Buszello¹⁶⁷, B. Butler⁵⁷, J.M. Butler²², A.I. Butt³, C.M. Buttar⁵³, J.M. Butterworth⁷⁷, P. Butti¹⁰⁶, W. Buttinger²⁸, A. Buzatu⁵³, M. Byszewski¹⁰, S. Cabrera Urbán¹⁶⁸, D. Caforio^{20a,20b}, O. Cakir^{4a}, P. Calafiura¹⁵, G. Calderini⁷⁹, P. Calfayan⁹⁹, R. Calkins¹⁰⁷, L.P. Caloba^{24a},

D. Calvet³⁴, S. Calvet³⁴, R. Camacho Toro⁴⁹, S. Camarda⁴², D. Cameron¹¹⁸, L.M. Caminada¹⁵, R. Caminal Armadans¹², S. Campana³⁰, M. Campanelli⁷⁷, A. Campoverde¹⁴⁹, V. Canale^{103a,103b}, A. Canepa^{160a}, J. Cantero⁸¹, R. Cantrill⁷⁶, T. Cao⁴⁰, M.D.M. Capeans Garrido³⁰, I. Caprini^{26a}, M. Caprini^{26a}, M. Capua^{37a,37b}, R. Caputo⁸², R. Cardarelli^{146c}, T. Carli³⁰, G. Carlino^{103a}, L. Carminati^{90a,90b}, S. Caron¹⁰⁵, E. Carquin^{32a}, G.D. Carrillo-Montoya^{146c}, A.A. Carter⁷⁵, J.R. Carter²⁸, J. Carvalho^{125a,125c}, D. Casadei⁷⁷, M.P. Casado¹², E. Castaneda-Miranda^{146b}, A. Castelli¹⁰⁶, V. Castillo Gimenez¹⁶⁸, N.F. Castro^{125a}, P. Catastini⁵⁷, A. Catinaccio³⁰, J.R. Catmore⁷¹, A. Cattai³⁰, G. Cattani^{134a,134b}, S. Caughron⁸⁹, V. Cavaliere¹⁶⁶, D. Cavalli^{90a}, M. Cavalli-Sforza¹², V. Cavasinni^{123a,123b}, F. Ceradini^{135a,135b}, B. Cerio⁴⁵, K. Cerny¹²⁸, A.S. Cerqueira^{24b}, A. Cerri¹⁵⁰, L. Cerrito⁷⁵, F. Cerutti¹⁵, M. Cerv³⁰, A. Cervelli¹⁷, S.A. Cetin^{19b}, A. Chafaq^{136a}, D. Chakraborty¹⁰⁷, I. Chalupkova¹²⁸, K. Chan³, P. Chang¹⁶⁶, B. Chapleau⁸⁶, J.D. Chapman²⁸, D. Charfeddine¹¹⁶, D.G. Charlton¹⁸, C.C. Chau¹⁵⁹, C.A. Chavez Barajas¹⁵⁰, S. Cheatham⁸⁶, A. Chegwiddden⁸⁹, S. Chekanov⁶, S.V. Chekulaev^{160a}, G.A. Chelkov⁶⁴, M.A. Chelstowska⁸⁸, C. Chen⁶³, H. Chen²⁵, K. Chen¹⁴⁹, L. Chen^{33d.g}, S. Chen^{33c}, X. Chen^{146c}, Y. Chen³⁵, H.C. Cheng⁸⁸, Y. Cheng³¹, A. Cheplakov⁶⁴, R. Cherkaoui El Moursli^{136e}, V. Chernyatin^{25,*}, E. Cheu⁷, L. Chevalier¹³⁷, V. Chiarella⁴⁷, G. Chiefari^{103a,103b}, J.T. Childers⁶, A. Chilingarov⁷¹, G. Chiodini^{72a}, A.S. Chisholm¹⁸, R.T. Chislett⁷⁷, A. Chitan^{26a}, M.V. Chizhov⁶⁴, S. Chouridou⁹, B.K.B. Chow⁹⁹, I.A. Christidi⁷⁷, D. Chromek-Burckhart³⁰, M.L. Chu¹⁵², J. Chudoba¹²⁶, L. Chytka¹¹⁴, G. Ciapetti^{133a,133b}, A.K. Ciftci^{4a}, R. Ciftci^{4a}, D. Cinca⁶², V. Cindro⁷⁴, A. Ciocio¹⁵, P. Cirkovic^{13b}, Z.H. Citron¹⁷³, M. Citterio^{90a}, M. Ciubancan^{26a}, A. Clark⁴⁹, P.J. Clark⁴⁶, R.N. Clarke¹⁵, W. Cleland¹²⁴, J.C. Clemens⁸⁴, B. Clement⁵⁵, C. Clement^{147a,147b}, Y. Coadou⁸⁴, M. Cobal^{165a,165c}, A. Cocco¹³⁹, J. Cochran⁶³, L. Coffey²³, J.G. Cogan¹⁴⁴, J. Coggeshall¹⁶⁶, B. Cole³⁵, S. Cole¹⁰⁷, A.P. Colijn¹⁰⁶, C. Collins-Tooth⁵³, J. Collot⁵⁵, T. Colombo^{58c}, G. Colon⁸⁵, G. Compostella¹⁰⁰, P. Conde Muño^{125a,125b}, E. Coniavitis¹⁶⁷, M.C. Conidi¹², S.H. Connell^{146b}, I.A. Connelly⁷⁶, S.M. Consonni^{90a,90b}, V. Consorti⁴⁸, S. Constantinescu^{26a}, C. Conta^{120a,120b}, G. Conti⁵⁷, F. Conventi^{103a,h}, M. Cooke¹⁵, B.D. Cooper⁷⁷, A.M. Cooper-Sarkar¹¹⁹, N.J. Cooper-Smith⁷⁶, K. Copic¹⁵, T. Cornelissen¹⁷⁶, M. Corradi^{20a}, F. Corrievau^{86,i}, A. Corso-Radu¹⁶⁴, A. Cortes-Gonzalez¹², G. Cortiana¹⁰⁰, G. Costa^{90a}, M.J. Costa¹⁶⁸, D. Costanzo¹⁴⁰, D. Côté⁸, G. Cottin²⁸, G. Cowan⁷⁶, B.E. Cox⁸³, K. Cranmer¹⁰⁹, G. Cree²⁹, S. Crépe-Renaudin⁵⁵, F. Crescioli⁷⁹, M. Crispin Ortuzar¹¹⁹, M. Cristinziani²¹, G. Crosetti^{37a,37b}, C.-M. Cuciuc^{26a}, C. Cuenca Almenar¹⁷⁷, T. Cuhadar Donszelmann¹⁴⁰, J. Cummings¹⁷⁷, M. Curatolo⁴⁷, C. Cuthbert¹⁵¹, H. Cziri¹⁴², P. Czodrowski³, Z. Czyczula¹⁷⁷, S. D'Auria⁵³, M. D'Onofrio⁷³, M.J. Da Cunha Sargedas De Sousa^{125a,125b}, C. Da Via⁸³, W. Dabrowski^{38a}, A. Dafinca¹¹⁹, T. Dai⁸⁸, O. Dale¹⁴, F. Dallaire⁹⁴, C. Dallapiccola⁸⁵, M. Dam³⁶, A.C. Daniells¹⁸, M. Dano Hoffmann¹³⁷, V. Dao¹⁰⁵, G. Darbo^{50a}, G.L. Darlea^{26c}, S. Darmora⁸, J.A. Dassoulas⁴², W. Davey²¹, C. David¹⁷⁰, T. Davidek¹²⁸, E. Davies^{119,c}, M. Davies⁹⁴, O. Davignon⁷⁹, A.R. Davison⁷⁷, P. Davison⁷⁷, Y. Davygora^{58a}, E. Dawe¹⁴³, I. Dawson¹⁴⁰, R.K. Daya-Ishmukhametova²³, K. De⁸, R. de Asmundis^{103a}, S. De Castro^{20a,20b}, S. De Cecco⁷⁹, J. de Graat⁹⁹, N. De Groot¹⁰⁵, P. de Jong¹⁰⁶, C. De La Taille¹¹⁶, H. De la Torre⁸¹, F. De Lorenzi⁶³, L. De Nooij¹⁰⁶, D. De Pedis^{133a}, A. De Salvo^{133a}, U. De Sanctis^{165a,165c}, A. De Santo¹⁵⁰, J.B. De Vivie De Regie¹¹⁶, G. De Zorzi^{133a,133b}, W.J. Dearnaley⁷¹, R. Debbe²⁵, C. Debenedetti⁴⁶, B. Dechenaux⁵⁵, D.V. Dedovich⁶⁴, J. Degenhardt¹²¹, I. Deigaard¹⁰⁶, J. Del Peso⁸¹, T. Del Prete^{123a,123b}, F. Deliot¹³⁷, M. Deliyergiyev⁷⁴, A. Dell'Acqua³⁰, L. Dell'Asta²², M. Dell'Orso^{123a,123b}, M. Della Pietra^{103a,h}, D. della Volpe⁴⁹, M. Delmastro⁵, P.A. Delsart⁵⁵, C. Deluca¹⁰⁶, S. Demers¹⁷⁷, M. Demichev⁶⁴, A. Demilly⁷⁹, S.P. Denisov¹²⁹, D. Derendarz³⁹, J.E. Derkaoui^{136d}, F. Derue⁷⁹, P. Dervan⁷³, K. Desch²¹, C. Deterre⁴², P.O. Deviveiros¹⁰⁶, A. Dewhurst¹³⁰, S. Dhaliwal¹⁰⁶, A. Di Ciaccio^{134a,134b}, L. Di Ciaccio⁵, A. Di Domenico^{133a,133b}, C. Di Donato^{103a,103b}, A. Di Girolamo³⁰, B. Di Girolamo³⁰, A. Di Mattia¹⁵³, B. Di Micco^{135a,135b}, R. Di Nardo⁴⁷, A. Di Simone⁴⁸, R. Di Sipio^{20a,20b}, D. Di Valentino²⁹, M.A. Diaz^{32a}, E.B. Diehl⁸⁸, J. Dietrich⁴², T.A. Dietzsch^{58a}, S. Diglio⁸⁷, A. Dimitrievska^{13a}, J. Dingfelder²¹, C. Dionisi^{133a,133b}, P. Dita^{26a}, S. Dita^{26a}, F. Dittus³⁰, F. Djama⁸⁴, T. Djobava^{51b}, M.A.B. do Vale^{24c}, A. Do Valle Wemans^{125a,125g}, T.K.O. Doan⁵, D. Dobos³⁰, E. Dobson⁷⁷, C. Doglioni⁴⁹, T. Doherty⁵³, T. Dohmae¹⁵⁶, J. Dolejsi¹²⁸, Z. Dolezal¹²⁸, B.A. Dolgoshein^{97,*}, M. Donadelli^{24d}, S. Donati^{123a,123b}, P. Dondero^{120a,120b}, J. Donini³⁴, J. Dopke³⁰, A. Doria^{103a}, A. Dos Anjos¹⁷⁴, M.T. Dova⁷⁰, A.T. Doyle⁵³, M. Dris¹⁰, J. Dubbert⁸⁸, S. Dube¹⁵, E. Dubreuil³⁴, E. Duchovni¹⁷³, G. Duckeck⁹⁹, O.A. Ducu^{26a}, D. Duda¹⁷⁶, A. Dudarev³⁰, F. Dudziak⁶³, L. Dufot¹¹⁶, L. Duguid⁷⁶, M. Dührssen³⁰, M. Dunford^{58a}, H. Duran Yildiz^{4a}, M. Düren⁵², A. Durglishvili^{51b}, M. Dwuznik^{38a}, M. Dyndal^{38a}, J. Ebke⁹⁹, W. Edson², N.C. Edwards⁴⁶, W. Ehrenfeld²¹, T. Eifert¹⁴⁴, G. Eigen¹⁴, K. Einsweiler¹⁵, T. Ekelof¹⁶⁷, M. El Kacimi^{136c}, M. Ellert¹⁶⁷, S. Elles⁵, F. Ellinghaus⁸², N. Ellis³⁰, J. Elmsheuser⁹⁹, M. Elsing³⁰, D. Emelianov¹³⁰, Y. Enari¹⁵⁶, O.C. Endner⁸², M. Endo¹¹⁷, R. Engelmann¹⁴⁹, J. Erdmann¹⁷⁷, A. Ereditato¹⁷, D. Eriksson^{147a}, G. Ernis¹⁷⁶, J. Ernst², M. Ernst²⁵, J. Ernwein¹³⁷, D. Errede¹⁶⁶, S. Errede¹⁶⁶, E. Ertel⁸², M. Escalier¹¹⁶, H. Esch⁴³, C. Escobar¹²⁴, B. Esposito⁴⁷, A.I. Etienne¹³⁷, E. Etzion¹⁵⁴, H. Evans⁶⁰, L. Fabbri^{20a,20b}, G. Facini³⁰, R.M. Fakhrutdinov¹²⁹, S. Falciano^{133a}, Y. Fang^{33a}, M. Fanti^{90a,90b}, A. Farbin⁸, A. Farilla^{135a}, T. Farooque¹², S. Farrell¹⁶⁴, S.M. Farrington¹⁷¹, P. Farthouat³⁰, F. Fassi¹⁶⁸, P. Fassnacht³⁰, D. Fassouliotis⁹, A. Favareto^{50a,50b}, L. Fayard¹¹⁶, P. Federic^{145a}, O.L. Fedin^{122.j}, W. Fedorko¹⁶⁹, M. Fehling-Kaschek⁴⁸, S. Feigl³⁰, L. Feligioni⁸⁴, C. Feng^{33d}, E.J. Feng⁶, H. Feng⁸⁸, A.B. Fenyuk¹²⁹, S. Fernandez Perez³⁰, W. Fernando⁶, S. Ferrag⁵³, J. Ferrando⁵³,

V. Ferrara⁴², A. Ferrari¹⁶⁷, P. Ferrari¹⁰⁶, R. Ferrari^{120a}, D.E. Ferreira de Lima⁵³, A. Ferrer¹⁶⁸, D. Ferrere⁴⁹, C. Ferretti⁸⁸, A. Ferretto Parodi^{50a,50b}, M. Fiascaris³¹, F. Fiedler⁸², A. Filipčić⁷⁴, M. Filipuzzi⁴², F. Filthaut¹⁰⁵, M. Fincke-Keeler¹⁷⁰, K.D. Finelli¹⁵¹, M.C.N. Fiolhais^{125a,125c}, L. Fiorini¹⁶⁸, A. Firan⁴⁰, J. Fischer¹⁷⁶, M.J. Fisher¹¹⁰, W.C. Fisher⁸⁹, E.A. Fitzgerald²³, M. Flechl⁴⁸, I. Fleck¹⁴², P. Fleischmann¹⁷⁵, S. Fleischmann¹⁷⁶, G.T. Fletcher¹⁴⁰, G. Fletcher⁷⁵, T. Flick¹⁷⁶, A. Floderus⁸⁰, L.R. Flores Castillo¹⁷⁴, A.C. Florez Bustos^{160b}, M.J. Flowerdew¹⁰⁰, A. Formica¹³⁷, A. Forti⁸³, D. Fortin^{160a}, D. Fournier¹¹⁶, H. Fox⁷¹, S. Fracchia¹², P. Francavilla¹², M. Franchini^{20a,20b}, S. Franchino³⁰, D. Francis³⁰, M. Franklin⁵⁷, S. Franz⁶¹, M. Fraternali^{120a,120b}, S.T. French²⁸, C. Friedrich⁴², F. Friedrich⁴⁴, D. Froidevaux³⁰, J.A. Frost²⁸, C. Fukunaga¹⁵⁷, E. Fullana Torregrosa⁸², B.G. Fulsom¹⁴⁴, J. Fuster¹⁶⁸, C. Gabaldon⁵⁵, O. Gabizon¹⁷³, A. Gabrielli^{20a,20b}, A. Gabrielli^{133a,133b}, S. Gadatsch¹⁰⁶, S. Gadomski⁴⁹, G. Gagliardi^{50a,50b}, P. Gagnon⁶⁰, C. Galea¹⁰⁵, B. Galhardo^{125a,125c}, E.J. Gallas¹¹⁹, V. Gallo¹⁷, B.J. Gallop¹³⁰, P. Gallus¹²⁷, G. Galster³⁶, K.K. Gan¹¹⁰, R.P. Gandrajula⁶², J. Gao^{33b,g}, Y.S. Gao^{144,e}, F.M. Garay Walls⁴⁶, F. Garberson¹⁷⁷, C. García¹⁶⁸, J.E. García Navarro¹⁶⁸, M. Garcia-Sciveres¹⁵, R.W. Gardner³¹, N. Garelli¹⁴⁴, V. Garonne³⁰, C. Gatti⁴⁷, G. Gaudio^{120a}, B. Gaur¹⁴², L. Gauthier⁹⁴, P. Gauzzi^{133a,133b}, I.L. Gavrilenko⁹⁵, C. Gay¹⁶⁹, G. Gaycken²¹, E.N. Gazis¹⁰, P. Ge^{33d}, Z. Gecse¹⁶⁹, C.N.P. Gee¹³⁰, D.A.A. Geerts¹⁰⁶, Ch. Geich-Gimbel²¹, K. Gellerstedt^{147a,147b}, C. Gemme^{50a}, A. Gemmell⁵³, M.H. Genest⁵⁵, S. Gentile^{133a,133b}, M. George⁵⁴, S. George⁷⁶, D. Gerbaudo¹⁶⁴, A. Gershon¹⁵⁴, H. Ghazlane^{136b}, N. Ghodbane³⁴, B. Giacobbe^{20a}, S. Giagu^{133a,133b}, V. Giangiobbe¹², P. Giannetti^{123a,123b}, F. Gianotti³⁰, B. Gibbard²⁵, S.M. Gibson⁷⁶, M. Gilchriese¹⁵, T.P.S. Gillam²⁸, D. Gillberg³⁰, D.M. Gingrich^{3,d}, N. Giokaris⁹, M.P. Giordani^{165a,165c}, R. Giordano^{103a,103b}, F.M. Giorgi¹⁶, P.F. Giraud¹³⁷, D. Giugni^{90a}, C. Giuliani⁴⁸, M. Giulini^{58b}, B.K. Gjelsten¹¹⁸, I. Gkialas^{155,k}, L.K. Gladilin⁹⁸, C. Glasman⁸¹, J. Glatzer³⁰, P.C.F. Glayshe⁴⁶, A. Glazov⁴², G.L. Glonti⁶⁴, M. Goblirsch-Kolb¹⁰⁰, J.R. Goddard⁷⁵, J. Godfrey¹⁴³, J. Godlewski³⁰, C. Goeringer⁸², S. Goldfarb⁸⁸, T. Golling¹⁷⁷, D. Golubkov¹²⁹, A. Gomes^{125a,125b,125d}, L.S. Gomez Fajardo⁴², R. Gonçalo^{125a}, J. Goncalves Pinto Firmino Da Costa⁴², L. Gonella²¹, S. González de la Hoz¹⁶⁸, G. Gonzalez Parra¹², M.L. Gonzalez Silva²⁷, S. Gonzalez-Sevilla⁴⁹, L. Goossens³⁰, P.A. Gorbounov⁹⁶, H.A. Gordon²⁵, I. Gorelov¹⁰⁴, G. Gorfine¹⁷⁶, B. Gorini³⁰, E. Gorini^{72a,72b}, A. Gorišek⁷⁴, E. Gornicki³⁹, A.T. Goshaw⁶, C. Gössling⁴³, M.I. Gostkin⁶⁴, M. Gouighri^{136a}, D. Goujdami^{136c}, M.P. Goulette⁴⁹, A.G. Goussiou¹³⁹, C. Goy⁵, S. Gozpinar²³, H.M.X. Grabas¹³⁷, L. Graber⁵⁴, I. Grabowska-Bold^{38a}, P. Grafström^{20a,20b}, K.-J. Grahn⁴², J. Gramling⁴⁹, E. Gramstad¹¹⁸, F. Grancagnolo^{72a}, S. Grancagnolo¹⁶, V. Grassi¹⁴⁹, V. Gratchev¹²², H.M. Gray³⁰, E. Graziani^{135a}, O.G. Grebenyuk¹²², Z.D. Greenwood^{78,l}, K. Gregersen³⁶, I.M. Gregor⁴², P. Grenier¹⁴⁴, J. Griffiths⁸, N. Grigalashvili⁶⁴, A.A. Grillo¹³⁸, K. Grimm⁷¹, S. Grinstein^{12,m}, Ph. Gris³⁴, Y.V. Grishkevich⁹⁸, J.-F. Grivaz¹¹⁶, J.P. Grohs⁴⁴, A. Grohsjean⁴², E. Gross¹⁷³, J. Grosse-Knetter⁵⁴, G.C. Grossi^{134a,134b}, J. Groth-Jensen¹⁷³, Z.J. Grout¹⁵⁰, K. Grybel¹⁴², L. Guan^{33b}, F. Guescini⁴⁹, D. Guest¹⁷⁷, O. Gueta¹⁵⁴, C. Guicheney³⁴, E. Guido^{50a,50b}, T. Guillemin¹¹⁶, S. Guindon², U. Gul⁵³, C. Gumpert⁴⁴, J. Gunther¹²⁷, J. Guo³⁵, S. Gupta¹¹⁹, P. Gutierrez¹¹², N.G. Gutierrez Ortiz⁵³, C. Gutschow⁷⁷, N. Guttman¹⁵⁴, C. Guyot¹³⁷, C. Gwenlan¹¹⁹, C.B. Gwilliam⁷³, A. Haas¹⁰⁹, C. Haber¹⁵, H.K. Hadavand⁸, N. Haddad^{136e}, P. Haefner²¹, S. Hageboeck²¹, Z. Hajduk³⁹, H. Hakobyan¹⁷⁸, M. Haleem⁴², D. Hall¹¹⁹, G. Halladjian⁸⁹, K. Hamacher¹⁷⁶, P. Hamal¹¹⁴, K. Hamano⁸⁷, M. Hamer⁵⁴, A. Hamilton^{146a}, S. Hamilton¹⁶², P.G. Hamnett⁴², L. Han^{33b}, K. Hanagaki¹¹⁷, K. Hanawa¹⁵⁶, M. Hance¹⁵, P. Hanke^{58a}, J.R. Hansen³⁶, J.B. Hansen³⁶, J.D. Hansen³⁶, P.H. Hansen³⁶, K. Hara¹⁶¹, A.S. Hard¹⁷⁴, T. Harenberg¹⁷⁶, S. Harkusha⁹¹, D. Harper⁸⁸, R.D. Harrington⁴⁶, O.M. Harris¹³⁹, P.F. Harrison¹⁷¹, F. Hartjes¹⁰⁶, A. Harvey⁵⁶, S. Hasegawa¹⁰², Y. Hasegawa¹⁴¹, A. Hasib¹¹², S. Hassani¹³⁷, S. Haug¹⁷, M. Hauschild³⁰, R. Hauser⁸⁹, M. Havranek¹²⁶, C.M. Hawkes¹⁸, R.J. Hawkings³⁰, A.D. Hawkins⁸⁰, T. Hayashi¹⁶¹, D. Hayden⁸⁹, C.P. Hays¹¹⁹, H.S. Hayward⁷³, S.J. Haywood¹³⁰, S.J. Head¹⁸, T. Heck⁸², V. Hedberg⁸⁰, L. Heelan⁸, S. Heim¹²¹, T. Heim¹⁷⁶, B. Heinemann¹⁵, L. Heinrich¹⁰⁹, S. Heisterkamp³⁶, J. Hejbal¹²⁶, L. Helary²², C. Heller⁹⁹, M. Heller³⁰, S. Hellman^{147a,147b}, D. Hellmich²¹, C. Helsen³⁰, J. Henderson¹¹⁹, R.C.W. Henderson⁷¹, C. Hengler⁴², A. Henrichs¹⁷⁷, A.M. Henriques Correia³⁰, S. Henrot-Versille¹¹⁶, C. Hensel⁵⁴, G.H. Herbert¹⁶, Y. Hernández Jiménez¹⁶⁸, R. Herrberg-Schubert¹⁶, G. Herten⁴⁸, R. Hertenberger⁹⁹, L. Hervas³⁰, G.G. Hesketh⁷⁷, N.P. Hesse¹⁰⁶, R. Hickling⁷⁵, E. Higón-Rodríguez¹⁶⁸, J.C. Hill²⁸, K.H. Hiller⁴², S. Hillert²¹, S.J. Hillier¹⁸, I. Hinchliffe¹⁵, E. Hines¹²¹, M. Hirose¹¹⁷, D. Hirschbuehl¹⁷⁶, J. Hobbs¹⁴⁹, N. Hod¹⁰⁶, M.C. Hodgkinson¹⁴⁰, P. Hodgson¹⁴⁰, A. Hoecker³⁰, M.R. Hoferkamp¹⁰⁴, J. Hoffman⁴⁰, D. Hoffmann⁸⁴, J.I. Hofmann^{58a}, M. Hohlfeld⁸², T.R. Holmes¹⁵, T.M. Hong¹²¹, L. Hooft van Huysduynen¹⁰⁹, J.-Y. Hostachy⁵⁵, S. Hou¹⁵², A. Hoummada^{136a}, J. Howard¹¹⁹, J. Howarth⁴², M. Hrabovsky¹¹⁴, I. Hristova¹⁶, J. Hrivnac¹¹⁶, T. Hryn'ova⁵, P.J. Hsu⁸², S.-C. Hsu¹³⁹, D. Hu³⁵, X. Hu²⁵, Y. Huang⁴², Z. Hubacek³⁰, F. Hubaut⁸⁴, F. Huegging²¹, T.B. Huffman¹¹⁹, E.W. Hughes³⁵, G. Hughes⁷¹, M. Huhtinen³⁰, T.A. Hülsing⁸², M. Hurwitz¹⁵, N. Huseynov^{64,b}, J. Huston⁸⁹, J. Huth⁵⁷, G. Iacobucci⁴⁹, G. Iakovidis¹⁰, I. Ibragimov¹⁴², L. Iconomidou-Fayard¹¹⁶, J. Idarraga¹¹⁶, E. Ideal¹⁷⁷, P. Iengo^{103a}, O. Igonkina¹⁰⁶, T. Iizawa¹⁷², Y. Ikegami⁶⁵, K. Ikematsu¹⁴², M. Ikeno⁶⁵, D. Iliadis¹⁵⁵, N. Ilic¹⁵⁹, Y. Inamaru⁶⁶, T. Ince¹⁰⁰, P. Ioannou⁹, M. Iodice^{135a}, K. Iordanidou⁹, V. Ippolito⁵⁷, A. Irles Quiles¹⁶⁸, C. Isaksson¹⁶⁷, M. Ishino⁶⁷, M. Ishitsuka¹⁵⁸, R. Ishmukhametov¹¹⁰, C. Issever¹¹⁹, S. Istin^{19a}, J.M. Iturbe Ponce⁸³, A.V. Ivashin¹²⁹, W. Iwanski³⁹, H. Iwasaki⁶⁵, J.M. Izen⁴¹, V. Izzo^{103a}, B. Jackson¹²¹, J.N. Jackson⁷³, M. Jackson⁷³,

P. Jackson¹, M.R. Jaekel³⁰, V. Jain², K. Jakobs⁴⁸, S. Jakobsen³⁶, T. Jakoubek¹²⁶, J. Jakubek¹²⁷, D.O. Jamin¹⁵², D.K. Jana⁷⁸, E. Jansen⁷⁷, H. Jansen³⁰, J. Janssen²¹, M. Janus¹⁷¹, G. Jarlskog⁸⁰, T. Javůrek⁴⁸, L. Jeanty¹⁵, G.-Y. Jeng¹⁵¹, D. Jennens⁸⁷, P. Jenni^{48,n}, J. Jentzsch⁴³, C. Jeske¹⁷¹, S. Jézéquel⁵, H. Ji¹⁷⁴, W. Ji⁸², J. Jia¹⁴⁹, Y. Jiang^{33b}, M. Jimenez Belenguer⁴², S. Jin^{33a}, A. Jinaru^{26a}, O. Jinnouchi¹⁵⁸, M.D. Joergensen³⁶, K.E. Johansson^{147a}, P. Johansson¹⁴⁰, K.A. Johns⁷, K. Jon-Anc^{147a,147b}, G. Jones¹⁷¹, R.W.L. Jones⁷¹, T.J. Jones⁷³, J. Jongmanns^{58a}, P.M. Jorge^{125a,125b}, K.D. Joshi⁸³, J. Jovicevic¹⁴⁸, X. Ju¹⁷⁴, C.A. Jung⁴³, R.M. Jungst³⁰, P. Jussel⁶¹, A. Juste Rozas^{12,m}, M. Kaci¹⁶⁸, A. Kaczmarek³⁹, M. Kado¹¹⁶, H. Kagan¹¹⁰, M. Kagan¹⁴⁴, E. Kajomovitz⁴⁵, S. Kama⁴⁰, N. Kanaya¹⁵⁶, M. Kaneda³⁰, S. Kaneti²⁸, T. Kanno¹⁵⁸, V.A. Kantserov⁹⁷, J. Kanzaki⁶⁵, B. Kaplan¹⁰⁹, A. Kapliy³¹, D. Kar⁵³, K. Karakostas¹⁰, N. Karastathis¹⁰, M. Karnevskiy⁸², S.N. Karpov⁶⁴, K. Karthik¹⁰⁹, V. Kartvelishvili⁷¹, A.N. Karyukhin¹²⁹, L. Kashif¹⁷⁴, G. Kasieczka^{58b}, R.D. Kass¹¹⁰, A. Kastanas¹⁴, Y. Kataoka¹⁵⁶, A. Katre⁴⁹, J. Katzy⁴², V. Kaushik⁷, K. Kawagoe⁶⁹, T. Kawamoto¹⁵⁶, G. Kawamura⁵⁴, S. Kazama¹⁵⁶, V.F. Kazanin¹⁰⁸, M.Y. Kazarinov⁶⁴, R. Keeler¹⁷⁰, P.T. Keener¹²¹, R. Kehoe⁴⁰, M. Keil⁵⁴, J.S. Keller⁴², H. Keoshkerian⁵, O. Kepka¹²⁶, B.P. Kerševan⁷⁴, S. Kersten¹⁷⁶, K. Kessoku¹⁵⁶, J. Keung¹⁵⁹, F. Khalil-zada¹¹, H. Khandanyan^{147a,147b}, A. Khanov¹¹³, A. Khodinov⁹⁷, A. Khomich^{58a}, T.J. Khoo²⁸, G. Khorauli²¹, A. Khoroshilov¹⁷⁶, V. Khovanskiy⁹⁶, E. Khramov⁶⁴, J. Khubua^{51b}, H.Y. Kim⁸, H. Kim^{147a,147b}, S.H. Kim¹⁶¹, N. Kimura¹⁷², O. Kind¹⁶, B.T. King⁷³, M. King¹⁶⁸, R.S.B. King¹¹⁹, S.B. King¹⁶⁹, J. Kirk¹³⁰, A.E. Kiryunin¹⁰⁰, T. Kishimoto⁶⁶, D. Kisielewska^{38a}, F. Kiss⁴⁸, T. Kitamura⁶⁶, T. Kittelmann¹²⁴, K. Kiuchi¹⁶¹, E. Kladiva^{145b}, M. Klein⁷³, U. Klein⁷³, K. Kleinknecht⁸², P. Klimek^{147a,147b}, A. Klimentov²⁵, R. Klingenberg⁴³, J.A. Klinger⁸³, E.B. Klinkby³⁶, T. Klioutchnikova³⁰, P.F. Klok¹⁰⁵, E.-E. Kluge^{58a}, P. Kluit¹⁰⁶, S. Kluth¹⁰⁰, E. Kneringer⁶¹, E.B.F.G. Knoop⁸⁴, A. Knue⁵³, T. Kobayashi¹⁵⁶, M. Kobel⁴⁴, M. Kocian¹⁴⁴, P. Kodys¹²⁸, P. Koevesarki²¹, T. Koffas²⁹, E. Koffeman¹⁰⁶, L.A. Kogan¹¹⁹, S. Kohlmann¹⁷⁶, Z. Kohout¹²⁷, T. Kohriki⁶⁵, T. Koi¹⁴⁴, H. Kolanoski¹⁶, I. Koletsou⁵, J. Koll⁸⁹, A.A. Komar^{95,*}, Y. Komori¹⁵⁶, T. Kondo⁶⁵, K. Köneke⁴⁸, A.C. König¹⁰⁵, S. König⁸², T. Kono^{65,o}, R. Konoplich^{109,p}, N. Konstantinidis⁷⁷, R. Kopeliainsky¹⁵³, S. Koperny^{38a}, L. Köpke⁸², A.K. Kopp⁴⁸, K. Korcyl³⁹, K. Kordas¹⁵⁵, A. Korn⁷⁷, A.A. Korol¹⁰⁸, I. Korolkov¹², E.V. Korolkova¹⁴⁰, V.A. Korotkov¹²⁹, O. Kortner¹⁰⁰, S. Kortner¹⁰⁰, V.V. Kostyukhin²¹, S. Kotov¹⁰⁰, V.M. Kotov⁶⁴, A. Kotwal⁴⁵, C. Kourkoumelis⁹, V. Kouskoura¹⁵⁵, A. Koutsman^{160a}, R. Kowalewski¹⁷⁰, T.Z. Kowalski^{38a}, W. Kozanecki¹³⁷, A.S. Kozhin¹²⁹, V. Kral¹²⁷, V.A. Kramarenko⁹⁸, G. Kramberger⁷⁴, D. Krasnopevtsev⁹⁷, M.W. Krasny⁷⁹, A. Krasznahorkay³⁰, J.K. Kraus²¹, A. Kravchenko²⁵, S. Kreiss¹⁰⁹, M. Kretz^{58c}, J. Kretzschmar⁷³, K. Kretzfeldt⁵², P. Krieger¹⁵⁹, K. Kroeninger⁵⁴, H. Kroha¹⁰⁰, J. Kroll¹²¹, J. Kroseberg²¹, J. Krstic^{13a}, U. Kruchonak⁶⁴, H. Krüger²¹, T. Kruker¹⁷, N. Krumnack⁶³, Z.V. Krumshteyn⁶⁴, A. Kruse¹⁷⁴, M.C. Kruse⁴⁵, M. Kruskal²², T. Kubota⁸⁷, S. Kудay^{4a}, S. Kuehn⁴⁸, A. Kugel^{58c}, A. Kuhl¹³⁸, T. Kuhl⁴², V. Kukhtin⁶⁴, Y. Kulchitsky⁹¹, S. Kuleshov^{32b}, M. Kuna^{133a,133b}, J. Kunkle¹²¹, A. Kupco¹²⁶, H. Kurashige⁶⁶, Y.A. Kurochkin⁹¹, R. Kurumida⁶⁶, V. Kus¹²⁶, E.S. Kuwertz¹⁴⁸, M. Kuze¹⁵⁸, J. Kvita¹⁴³, A. La Rosa⁴⁹, L. La Rotonda^{37a,37b}, L. Labarga⁸¹, C. Lacasta¹⁶⁸, F. Lacava^{133a,133b}, J. Lacey²⁹, H. Lacker¹⁶, D. Lacour⁷⁹, V.R. Lacuesta¹⁶⁸, E. Ladygin⁶⁴, R. Lafaye⁵, B. Laforge⁷⁹, T. Lagouri¹⁷⁷, S. Lai⁴⁸, H. Laier^{58a}, L. Lambourne⁷⁷, S. Lammers⁶⁰, C.L. Lampen⁷, W. Lampl⁷, E. Lançon¹³⁷, U. Landgraf⁴⁸, M.P.J. Landon⁷⁵, V.S. Lang^{58a}, C. Lange⁴², A.J. Lankford¹⁶⁴, F. Lanni²⁵, K. Lantzsck³⁰, S. Laplace⁷⁹, C. Lapoire²¹, J.F. Laporte¹³⁷, T. Lari^{90a}, M. Lassnig³⁰, P. Laurelli⁴⁷, V. Lavorini^{37a,37b}, W. Lavrijsen¹⁵, A.T. Law¹³⁸, P. Laycock⁷³, B.T. Le⁵⁵, O. Le Dortz⁷⁹, E. Le Guirriec⁸⁴, E. Le Menedeu¹², T. LeCompte⁶, F. Ledroit-Guillon⁵⁵, C.A. Lee¹⁵², H. Lee¹⁰⁶, J.S.H. Lee¹¹⁷, S.C. Lee¹⁵², L. Lee¹⁷⁷, G. Lefebvre⁷⁹, M. Lefebvre¹⁷⁰, F. Legger⁹⁹, C. Leggett¹⁵, A. Lehan⁷³, M. Lehmacher²¹, G. Lehmann Miotto³⁰, X. Lei⁷, A.G. Leister¹⁷⁷, M.A.L. Leite^{24d}, R. Leitner¹²⁸, D. Lellouch¹⁷³, B. Lemmer⁵⁴, K.J.C. Leney⁷⁷, T. Lenz¹⁰⁶, G. Lenzen¹⁷⁶, B. Lenzi³⁰, R. Leone⁷, K. Leonhardt⁴⁴, S. Leontsinis¹⁰, C. Leroy⁹⁴, C.G. Lester²⁸, C.M. Lester¹²¹, J. Levêque⁵, D. Levin⁸⁸, L.J. Levinson¹⁷³, M. Levy¹⁸, A. Lewis¹¹⁹, G.H. Lewis¹⁰⁹, A.M. Leyko²¹, M. Leyton⁴¹, B. Li^{33b,q}, B. Li⁸⁴, H. Li¹⁴⁹, H.L. Li³¹, S. Li⁴⁵, X. Li⁸⁸, Y. Li^{33c,r}, Z. Liang^{119,s}, H. Liao³⁴, B. Liberti^{134a}, P. Lichard³⁰, K. Lie¹⁶⁶, J. Liebal²¹, W. Liebig¹⁴, C. Limbach²¹, A. Limosani⁸⁷, M. Limper⁶², S.C. Lin^{152,t}, F. Linde¹⁰⁶, B.E. Lindquist¹⁴⁹, J.T. Linnemann⁸⁹, E. Lipeles¹²¹, A. Lipniacka¹⁴, M. Lisovsky⁴², T.M. Liss¹⁶⁶, D. Lissauer²⁵, A. Lister¹⁶⁹, A.M. Litke¹³⁸, B. Liu¹⁵², D. Liu¹⁵², J.B. Liu^{33b}, K. Liu^{33b,u}, L. Liu⁸⁸, M. Liu⁴⁵, M. Liu^{33b}, Y. Liu^{33b}, M. Livan^{120a,120b}, S.S.A. Livermore¹¹⁹, A. Lleres⁵⁵, J. Llorente Merino⁸¹, S.L. Lloyd⁷⁵, F. Lo Sterzo¹⁵², E. Lobodzinska⁴², P. Loch⁷, W.S. Lockman¹³⁸, T. Loddenkoetter²¹, F.K. Loebinger⁸³, A.E. Loeschall-Jensen³⁶, A. Loginov¹⁷⁷, C.W. Loh¹⁶⁹, T. Lohse¹⁶, K. Lohwasser⁴⁸, M. Lokajicek¹²⁶, V.P. Lombardo⁵, J.D. Long⁸⁸, R.E. Long⁷¹, L. Lopes^{125a}, D. Lopez Mateos⁵⁷, B. Lopez Paredes¹⁴⁰, J. Lorenz⁹⁹, N. Lorenzo Martinez⁶⁰, M. Losada¹⁶³, P. Loscutoff¹⁵, M.J. Losty^{160a,*}, X. Lou⁴¹, A. Lounis¹¹⁶, J. Love⁶, P.A. Love⁷¹, A.J. Lowe^{144,e}, F. Lu^{33a}, H.J. Lubatti¹³⁹, C. Luci^{133a,133b}, A. Lucotte⁵⁵, F. Luehring⁶⁰, W. Lukas⁶¹, L. Luminari^{133a}, O. Lundberg^{147a,147b}, B. Lund-Jensen¹⁴⁸, M. Lungwitz⁸², D. Lynn²⁵, R. Lysak¹²⁶, E. Lytken⁸⁰, H. Ma²⁵, L.L. Ma^{33d}, G. Maccarrone⁴⁷, A. Macchiolo¹⁰⁰, B. Maček⁷⁴, J. Machado Miguens^{125a,125b}, D. Macina³⁰, D. Madaffari⁸⁴, R. Madar⁴⁸, H.J. Maddocks⁷¹, W.F. Mader⁴⁴, A. Madsen¹⁶⁷, M. Maeno⁸, T. Maeno²⁵, E. Magradze⁵⁴, K. Mahboubi⁴⁸, J. Mahlstedt¹⁰⁶, S. Mahmoud⁷³, C. Maiani¹³⁷, C. Maidantchik^{24a}, A. Maio^{125a,125b,125d}, S. Majewski¹¹⁵, Y. Makida⁶⁵, N. Makovec¹¹⁶, P. Mal^{137,v}, B. Malaescu⁷⁹, Pa. Malecki³⁹,

V.P. Maleev¹²², F. Malek⁵⁵, U. Mallik⁶², D. Malon⁶, C. Malone¹⁴⁴, S. Maltezos¹⁰, V.M. Malyshev¹⁰⁸, S. Malyukov³⁰, J. Mamuzic^{13b}, B. Mandelli³⁰, L. Mandelli^{90a}, I. Mandić⁷⁴, R. Mandrysch⁶², J. Maneira^{125a,125b}, A. Manfredini¹⁰⁰, L. Manhaes de Andrade Filho^{24b}, J.A. Manjarres Ramos^{160b}, A. Mann⁹⁹, P.M. Manning¹³⁸, A. Manousakis-Katsikakis⁹, B. Mansoulie¹³⁷, R. Mantifel⁸⁶, L. Mapelli³⁰, L. March¹⁶⁸, J.F. Marchand²⁹, F. Marchese^{134a,134b}, G. Marchiori⁷⁹, M. Marcisovsky¹²⁶, C.P. Marino¹⁷⁰, C.N. Marques^{125a}, F. Marroquin^{24a}, S.P. Marsden⁸³, Z. Marshall¹⁵, L.F. Marti¹⁷, S. Marti-Garcia¹⁶⁸, B. Martin³⁰, B. Martin⁸⁹, J.P. Martin⁹⁴, T.A. Martin¹⁷¹, V.J. Martin⁴⁶, B. Martin dit Latour⁴⁹, H. Martinez¹³⁷, M. Martinez^{12,m}, S. Martin-Haugh¹³⁰, A.C. Martyniuk⁷⁷, M. Marx¹³⁹, F. Marzano^{133a}, A. Marzin³⁰, L. Masetti⁸², T. Mashimo¹⁵⁶, R. Mashinistov⁹⁵, J. Masik⁸³, A.L. Maslennikov¹⁰⁸, I. Massa^{20a,20b}, N. Massol⁵, P. Mastrandrea¹⁴⁹, A. Mastroberardino^{37a,37b}, T. Masubuchi¹⁵⁶, P. Matricon¹¹⁶, H. Matsunaga¹⁵⁶, T. Matsushita⁶⁶, P. Mättig¹⁷⁶, S. Mättig⁴², J. Mattmann⁸², J. Maurer^{26a}, S.J. Maxfield⁷³, D.A. Maximov^{108,f}, R. Mazini¹⁵², L. Mazzaferro^{134a,134b}, G. Mc Goldrick¹⁵⁹, S.P. Mc Kee⁸⁸, A. McCarn⁸⁸, R.L. McCarthy¹⁴⁹, T.G. McCarthy²⁹, N.A. McCubbin¹³⁰, K.W. McFarlane^{56,*}, J.A. MCFayden⁷⁷, G. Mchedlidze⁵⁴, T. McLaughlan¹⁸, S.J. McMahon¹³⁰, R.A. McPherson^{170,i}, A. Meade⁸⁵, J. Mechnich¹⁰⁶, M. Medinnis⁴², S. Meehan³¹, R. Meera-Lebbai¹¹², S. Mehlhase³⁶, A. Mehta⁷³, K. Meier^{58a}, C. Meineck⁹⁹, B. Meirose⁸⁰, C. Melachrinou³¹, B.R. Mellado Garcia^{146c}, F. Meloni^{90a,90b}, L. Mendoza Navas¹⁶³, A. Mengarelli^{20a,20b}, S. Menke¹⁰⁰, E. Meoni¹⁶², K.M. Mercurio⁵⁷, S. Mergelmeyer²¹, N. Meric¹³⁷, P. Mermod⁴⁹, L. Merola^{103a,103b}, C. Meroni^{90a}, F.S. Merritt³¹, H. Merritt¹¹⁰, A. Messina^{30,w}, J. Metcalfe²⁵, A.S. Mete¹⁶⁴, C. Meyer⁸², C. Meyer³¹, J-P. Meyer¹³⁷, J. Meyer³⁰, R.P. Middleton¹³⁰, S. Migas⁷³, L. Mijović¹³⁷, G. Mikenberg¹⁷³, M. Mikestikova¹²⁶, M. Mikuz⁷⁴, D.W. Miller³¹, C. Mills⁴⁶, A. Milov¹⁷³, D.A. Milstead^{147a,147b}, D. Milstein¹⁷³, A.A. Minaenko¹²⁹, M. Miñano Moya¹⁶⁸, I.A. Minashvili⁶⁴, A.I. Mincer¹⁰⁹, B. Mindur^{38a}, M. Mineev⁶⁴, Y. Ming¹⁷⁴, L.M. Mir¹², G. Mirabelli^{133a}, T. Mitani¹⁷², J. Mitrevski⁹⁹, V.A. Mitsou¹⁶⁸, S. Mitsui⁶⁵, A. Miucci⁴⁹, P.S. Miyagawa¹⁴⁰, J.U. Mjörnmark⁸⁰, T. Moa^{147a,147b}, K. Mochizuki⁸⁴, V. Moeller²⁸, S. Mohapatra³⁵, W. Mohr⁴⁸, S. Molander^{147a,147b}, R. Moles-Valls¹⁶⁸, K. Mönig⁴², C. Monini⁵⁵, J. Monk³⁶, E. Monnier⁸⁴, J. Montejo Berlingen¹², F. Monticelli⁷⁰, S. Monzani^{133a,133b}, R.W. Moore³, C. Mora Herrera⁴⁹, A. Moraes⁵³, N. Morange⁶², J. Morel⁵⁴, D. Moreno⁸², M. Moreno Llacer⁵⁴, P. Morettini^{50a}, M. Morgenstern⁴⁴, M. Morii⁵⁷, S. Moritz⁸², A.K. Morley¹⁴⁸, G. Mornacchi³⁰, J.D. Morris⁷⁵, L. Morvaj¹⁰², H.G. Moser¹⁰⁰, M. Mosidze^{51b}, J. Moss¹¹⁰, R. Mount¹⁴⁴, E. Mountricha²⁵, S.V. Mouraviev^{95,*}, E.J.W. Moyses⁸⁵, S. Muanza⁸⁴, R.D. Mudd¹⁸, F. Mueller^{58a}, J. Mueller¹²⁴, K. Mueller²¹, T. Mueller²⁸, T. Mueller⁸², D. Muenstermann⁴⁹, Y. Munwes¹⁵⁴, J.A. Murillo Quijada¹⁸, W.J. Murray^{171,130}, E. Musto¹⁵³, A.G. Myagkov^{129,x}, M. Myska¹²⁶, O. Nackenhorst⁵⁴, J. Nadal⁵⁴, K. Nagai⁶¹, R. Nagai¹⁵⁸, Y. Nagai⁸⁴, K. Nagano⁶⁵, A. Nagarkar¹¹⁰, Y. Nagasaka⁵⁹, M. Nagel¹⁰⁰, A.M. Nairz³⁰, Y. Nakahama³⁰, K. Nakamura⁶⁵, T. Nakamura¹⁵⁶, I. Nakano¹¹¹, H. Namasivayam⁴¹, G. Nanava²¹, R. Narayan^{58b}, T. Nattermann²¹, T. Naumann⁴², G. Navarro¹⁶³, R. Nayyar⁷, H.A. Neal⁸⁸, P.Yu. Nechaeva⁹⁵, T.J. Neep⁸³, A. Negri^{120a,120b}, G. Negri³⁰, M. Negrini^{20a}, S. Nektarijevic⁴⁹, A. Nelson¹⁶⁴, T.K. Nelson¹⁴⁴, S. Nemecek¹²⁶, P. Nemethy¹⁰⁹, A.A. Nepomuceno^{24a}, M. Nessi^{30,y}, M.S. Neubauer¹⁶⁶, M. Neumann¹⁷⁶, R.M. Neves¹⁰⁹, P. Nevski²⁵, F.M. Newcomer¹²¹, P.R. Newman¹⁸, D.H. Nguyen⁶, R.B. Nickerson¹¹⁹, R. Nicolaidou¹³⁷, B. Nicquevert³⁰, J. Nielsen¹³⁸, N. Nikiforou³⁵, A. Nikiforov¹⁶, V. Nikolaenko^{129,x}, I. Nikolic-Audit⁷⁹, K. Nikolics⁴⁹, K. Nikolopoulos¹⁸, P. Nilsson⁸, Y. Ninomiya¹⁵⁶, A. Nisati^{133a}, R. Nisius¹⁰⁰, T. Nobe¹⁵⁸, L. Nodulman⁶, M. Nomachi¹¹⁷, I. Nomidis¹⁵⁵, S. Norberg¹¹², M. Nordberg³⁰, J. Novakova¹²⁸, S. Nowak¹⁰⁰, M. Nozaki⁶⁵, L. Nozka¹¹⁴, K. Ntekas¹⁰, G. Nunes Hanninger⁸⁷, T. Nunnemann⁹⁹, E. Nurse⁷⁷, F. Nuti⁸⁷, B.J. O'Brien⁴⁶, F. O'grady⁷, D.C. O'Neil¹⁴³, V. O'Shea⁵³, F.G. Oakham^{29,d}, H. Oberlack¹⁰⁰, T. Obermann²¹, J. Ocariz⁷⁹, A. Ochi⁶⁶, M.I. Ochoa⁷⁷, S. Oda⁶⁹, S. Odaka⁶⁵, H. Ogren⁶⁰, A. Oh⁸³, S.H. Oh⁴⁵, C.C. Ohm³⁰, H. Ohman¹⁶⁷, T. Ohshima¹⁰², W. Okamura¹¹⁷, H. Okawa²⁵, Y. Okumura³¹, T. Okuyama¹⁵⁶, A. Olariu^{26a}, A.G. Olchevski⁶⁴, S.A. Olivares Pino⁴⁶, D. Oliveira Damazio²⁵, E. Oliver Garcia¹⁶⁸, D. Olivito¹²¹, A. Olszewski³⁹, J. Olszowska³⁹, A. Onofre^{125a,125e}, P.U.E. Onyisi^{31,z}, C.J. Oram^{160a}, M.J. Oreglia³¹, Y. Oren¹⁵⁴, D. Orestano^{135a,135b}, N. Orlando^{72a,72b}, C. Oropeza Barrera⁵³, R.S. Orr¹⁵⁹, B. Osculati^{50a,50b}, R. Ospanov¹²¹, G. Otero y Garzon²⁷, H. Otono⁶⁹, M. Ouchrif^{136d}, E.A. Ouellette¹⁷⁰, F. Ould-Saada¹¹⁸, A. Ouraou¹³⁷, K.P. Oussoren¹⁰⁶, Q. Ouyang^{33a}, A. Ovcharova¹⁵, M. Owen⁸³, V.E. Ozcan^{19a}, N. Ozturk⁸, K. Pachal¹¹⁹, A. Pacheco Pages¹², C. Padilla Aranda¹², M. Pagáčová⁴⁸, S. Pagan Griso¹⁵, E. Paganis¹⁴⁰, C. Pahl¹⁰⁰, F. Paige²⁵, P. Pais⁸⁵, K. Pajchel¹¹⁸, G. Palacino^{160b}, S. Palestini³⁰, D. Pallin³⁴, A. Palma^{125a,125b}, J.D. Palmer¹⁸, Y.B. Pan¹⁷⁴, E. Panagiotopoulou¹⁰, J.G. Panduro Vazquez⁷⁶, P. Pani¹⁰⁶, N. Panikashvili⁸⁸, S. Panitkin²⁵, D. Pantea^{26a}, L. Paolozzi^{134a,134b}, Th.D. Papadopoulou¹⁰, K. Papageorgiou^{155,k}, A. Paramonov⁶, D. Paredes Hernandez³⁴, M.A. Parker²⁸, F. Parodi^{50a,50b}, J.A. Parsons³⁵, U. Parzefall⁴⁸, E. Pasqualucci^{133a}, S. Passaggio^{50a}, A. Passeri^{135a}, F. Pastore^{135a,135b,*}, Fr. Pastore⁷⁶, G. Pásztor^{49,aa}, S. Patariaia¹⁷⁶, N.D. Patel¹⁵¹, J.R. Pater⁸³, S. Patricelli^{103a,103b}, T. Pauly³⁰, J. Pearce¹⁷⁰, M. Pedersen¹¹⁸, S. Pedraza Lopez¹⁶⁸, R. Pedro^{125a,125b}, S.V. Peleganchuk¹⁰⁸, D. Pelikan¹⁶⁷, H. Peng^{33b}, B. Penning³¹, J. Penwell⁶⁰, D.V. Perepelitsa²⁵, E. Perez Codina^{160a}, M.T. Pérez García-Están¹⁶⁸, V. Perez Reale³⁵, L. Perini^{90a,90b}, H. Pernegger³⁰, R. Perrino^{72a}, R. Peschke⁴², V.D. Peshekhonov⁶⁴, K. Peters³⁰, R.F.Y. Peters⁸³, B.A. Petersen⁸⁷, J. Petersen³⁰, T.C. Petersen³⁶, E. Petit⁴², A. Petridis^{147a,147b}, C. Petridou¹⁵⁵, E. Petrolo^{133a}, F. Petrucci^{135a,135b}, M. Petteni¹⁴³, N.E. Pettersson¹⁵⁸,

R. Pezoa^{32b}, P.W. Phillips¹³⁰, G. Piacquadio¹⁴⁴, E. Pianori¹⁷¹, A. Picazio⁴⁹, E. Piccaro⁷⁵, M. Piccinini^{20a,20b}, S.M. Piec⁴², R. Piegai²⁷, D.T. Pignotti¹¹⁰, J.E. Pilcher³¹, A.D. Pilkington⁷⁷, J. Pina^{125a,125b,125d}, M. Pinamonti^{165a,165c,ab}, A. Pinder¹¹⁹, J.L. Pinfold³, A. Pingel³⁶, B. Pinto^{125a}, S. Pires⁷⁹, C. Pizio^{90a,90b}, M.-A. Pleier²⁵, V. Pleskot¹²⁸, E. Plotnikova⁶⁴, P. Plucinski^{147a,147b}, S. Poddar^{58a}, F. Podlyski³⁴, R. Poettgen⁸², L. Poggioli¹¹⁶, D. Pohl²¹, M. Pohl⁴⁹, G. Polesello^{120a}, A. Policicchio^{37a,37b}, R. Polifka¹⁵⁹, A. Polini^{20a}, C.S. Pollard⁴⁵, V. Polychronakos²⁵, K. Pommès³⁰, L. Pontecorvo^{133a}, B.G. Pope⁸⁹, G.A. Popeneciu^{26b}, D.S. Popovic^{13a}, A. Poppleton³⁰, X. Portell Bueso¹², G.E. Pospelov¹⁰⁰, S. Pospisil¹²⁷, K. Potamianos¹⁵, I.N. Potrap⁶⁴, C.J. Potter¹⁵⁰, C.T. Potter¹¹⁵, G. Poulard³⁰, J. Poveda⁶⁰, V. Pozdnyakov⁶⁴, R. Prabhu⁷⁷, P. Pralavorio⁸⁴, A. Pranko¹⁵, S. Prasad³⁰, R. Pravahan⁸, S. Prell⁶³, D. Price⁸³, J. Price⁷³, L.E. Price⁶, D. Prieur¹²⁴, M. Primavera^{72a}, M. Proissl⁴⁶, K. Prokofiev⁴⁷, F. Prokoshin^{32b}, E. Protopapadaki¹³⁷, S. Protopopescu²⁵, J. Proudfoot⁶, M. Przybycien^{38a}, H. Przysieszniak⁵, E. Ptacek¹¹⁵, E. Pueschel⁸⁵, D. Puldon¹⁴⁹, M. Purohit^{25,ac}, P. Puzo¹¹⁶, Y. Pylypchenko⁶², J. Qian⁸⁸, G. Qin⁵³, A. Quadt⁵⁴, D.R. Quarrie¹⁵, W.B. Quayle^{165a,165b}, D. Quilty⁵³, A. Qureshi^{160b}, V. Radeka²⁵, V. Radescu⁴², S.K. Radhakrishnan¹⁴⁹, P. Radloff¹¹⁵, P. Rados⁸⁷, F. Ragusa^{90a,90b}, G. Rahal¹⁷⁹, S. Rajagopalan²⁵, M. Rammensee³⁰, M. Rammes¹⁴², A.S. Randle-Conde⁴⁰, C. Rangel-Smith⁷⁹, K. Rao¹⁶⁴, F. Rauscher⁹⁹, T.C. Rave⁴⁸, T. Ravenscroft⁵³, M. Raymond³⁰, A.L. Read¹¹⁸, D.M. Rebuffi^{120a,120b}, A. Redelbach¹⁷⁵, G. Redlinger²⁵, R. Reece¹³⁸, K. Reeves⁴¹, L. Rehnisch¹⁶, A. Reinsch¹¹⁵, H. Reisin²⁷, M. Relich¹⁶⁴, C. Rembser³⁰, Z.L. Ren¹⁵², A. Renaud¹¹⁶, M. Rescigno^{133a}, S. Resconi^{90a}, B. Resende¹³⁷, P. Reznicek¹²⁸, R. Rezvani⁹⁴, R. Richter¹⁰⁰, M. Ridel⁷⁹, P. Rieck¹⁶, M. Rijssenbeek¹⁴⁹, A. Rimoldi^{120a,120b}, L. Rinaldi^{20a}, E. Ritsch⁶¹, I. Riu¹², F. Rizatdinova¹¹³, E. Rizvi⁷⁵, S.H. Robertson^{86,i}, A. Robichaud-Veronneau¹¹⁹, D. Robinson²⁸, J.E.M. Robinson⁸³, A. Robson⁵³, C. Roda^{123a,123b}, L. Rodrigues³⁰, S. Roe³⁰, O. Röhne¹¹⁸, S. Rolli¹⁶², A. Romaniouk⁹⁷, M. Romano^{20a,20b}, G. Romeo²⁷, E. Romero Adam¹⁶⁸, N. Rompotis¹³⁹, L. Roos⁷⁹, E. Ros¹⁶⁸, S. Rosati^{133a}, K. Rosbach⁴⁹, A. Rose¹⁵⁰, M. Rose⁷⁶, P.L. Rosendahl¹⁴, O. Rosenthal¹⁴², V. Rossetti^{147a,147b}, E. Rossi^{103a,103b}, L.P. Rossi^{50a}, R. Rosten¹³⁹, M. Rotaru^{26a}, I. Roth¹⁷³, J. Rothberg¹³⁹, D. Rousseau¹¹⁶, C.R. Royon¹³⁷, A. Rozanov⁸⁴, Y. Rozen¹⁵³, X. Ruan^{146c}, F. Rubbo¹², I. Rubinskiy⁴², V.I. Rud⁹⁸, C. Rudolph⁴⁴, M.S. Rudolph¹⁵⁹, F. Rühr⁴⁸, A. Ruiz-Martinez⁶³, Z. Rurikova⁴⁸, N.A. Rusakovich⁶⁴, A. Ruschke⁹⁹, J.P. Rutherford⁷, N. Ruthmann⁴⁸, Y.F. Ryabov¹²², M. Rybar¹²⁸, G. Rybkin¹¹⁶, N.C. Ryder¹¹⁹, A.F. Saavedra¹⁵¹, S. Sacerdoti²⁷, A. Saddique³, I. Sadeh¹⁵⁴, H.F.-W. Sadrozinski¹³⁸, R. Sadykov⁶⁴, F. Safai Tehrani^{133a}, H. Sakamoto¹⁵⁶, Y. Sakurai¹⁷², G. Salamanna⁷⁵, A. Salamon^{134a}, M. Saleem¹¹², D. Salek¹⁰⁶, P.H. Sales De Bruin¹³⁹, D. Salihagic¹⁰⁰, A. Salmikov¹⁴⁴, J. Salt¹⁶⁸, B.M. Salvachua Ferrando⁶, D. Salvatore^{37a,37b}, F. Salvatore¹⁵⁰, A. Salvucci¹⁰⁵, A. Salzburger³⁰, D. Sampsonidis¹⁵⁵, A. Sanchez^{103a,103b}, J. Sánchez¹⁶⁸, V. Sanchez Martinez¹⁶⁸, H. Sandaker¹⁴, H.G. Sander⁸², M.P. Sanders⁹⁹, M. Sandhoff¹⁷⁶, T. Sandoval²⁸, C. Sandoval¹⁶³, R. Sandstroem¹⁰⁰, D.P.C. Sankey¹³⁰, A. Sansoni⁴⁷, C. Santoni³⁴, R. Santonico^{134a,134b}, H. Santos^{125a}, I. Santoyo Castillo¹⁵⁰, K. Sapp¹²⁴, A. Sapronov⁶⁴, J.G. Saraiva^{125a,125d}, B. Sarrazin²¹, G. Sartisoehn¹⁷⁶, O. Sasaki⁶⁵, Y. Sasaki¹⁵⁶, I. Satsounkevitch⁹¹, G. Sauvage^{5,*}, E. Sauvan⁵, P. Savard^{159,d}, D.O. Savu³⁰, C. Sawyer¹¹⁹, L. Sawyer^{78,l}, D.H. Saxon⁵³, J. Saxon¹²¹, C. Sbarra^{20a}, A. Sbrizzi³, T. Scanlon³⁰, D.A. Scannicchio¹⁶⁴, M. Scarcella¹⁵¹, J. Schaarschmidt¹⁷³, P. Schacht¹⁰⁰, D. Schaefer¹²¹, R. Schaefer⁴², A. Schaelicke⁴⁶, S. Schaepe²¹, S. Schaetzel^{58b}, U. Schäfer⁸², A.C. Schaffer¹¹⁶, D. Schaile⁹⁹, R.D. Schamberger¹⁴⁹, V. Scharf^{58a}, V.A. Schegelsky¹²², D. Scheirich¹²⁸, M. Schernau¹⁶⁴, M.I. Scherzer³⁵, C. Schiavi^{50a,50b}, J. Schieck⁹⁹, C. Schillo⁴⁸, M. Schioppa^{37a,37b}, S. Schlenker³⁰, E. Schmidt⁴⁸, K. Schmieden³⁰, C. Schmitt⁸², C. Schmitt⁹⁹, S. Schmitt^{58b}, B. Schneider¹⁷, Y.J. Schnellbach⁷³, U. Schnoor⁴⁴, L. Schoeffel¹³⁷, A. Schoening^{58b}, B.D. Schoenrock⁸⁹, A.L.S. Schorlemmer⁵⁴, M. Schott⁸², D. Schouten^{160a}, J. Schovancova²⁵, M. Schram⁸⁶, S. Schramm¹⁵⁹, M. Schreyer¹⁷⁵, C. Schroeder⁸², N. Schuh⁸², M.J. Schultens²¹, H.-C. Schultz-Coulon^{58a}, H. Schulz¹⁶, M. Schumacher⁴⁸, B.A. Schumm¹³⁸, Ph. Schune¹³⁷, A. Schwartzman¹⁴⁴, Ph. Schwegler¹⁰⁰, Ph. Schwemling¹³⁷, R. Schwienhorst⁸⁹, J. Schwindling¹³⁷, T. Schwindt²¹, M. Schwoerer⁵, F.G. Sciacca¹⁷, E. Scifo¹¹⁶, G. Sciolla²³, W.G. Scott¹³⁰, F. Scuri^{123a,123b}, F. Scutti²¹, J. Searcy⁸⁸, G. Sedov⁴², E. Sedykh¹²², S.C. Seidel¹⁰⁴, A. Seiden¹³⁸, F. Seifert¹²⁷, J.M. Seixas^{24a}, G. Sekhniaidze^{103a}, S.J. Sekula⁴⁰, K.E. Selbach⁴⁶, D.M. Seliverstov^{122,*}, G. Sellers⁷³, N. Semprini-Cesari^{20a,20b}, C. Serfon³⁰, L. Serin¹¹⁶, L. Serkin⁵⁴, T. Serre⁸⁴, R. Seuster^{160a}, H. Severini¹¹², F. Sforza¹⁰⁰, A. Sfyrila³⁰, E. Shabalina⁵⁴, M. Shamim¹¹⁵, L.Y. Shan^{33a}, J.T. Shank²², Q.T. Shao⁸⁷, M. Shapiro¹⁵, P.B. Shatalov⁹⁶, K. Shaw^{165a,165b}, P. Sherwood⁷⁷, S. Shimizu⁶⁶, C.O. Shimmin¹⁶⁴, M. Shimojima¹⁰¹, T. Shin⁵⁶, M. Shiyakova⁶⁴, A. Shmeleva⁹⁵, M.J. Shochet³¹, D. Short¹¹⁹, S. Shrestha⁶³, E. Shulga⁹⁷, M.A. Shupe⁷, S. Shushkevich⁴², P. Sicho¹²⁶, D. Sidorov¹¹³, A. Sidoti^{133a}, F. Siegert⁴⁴, Dj. Sijacki^{13a}, O. Silbert¹⁷³, J. Silva^{125a,125d}, Y. Silver¹⁵⁴, D. Silverstein¹⁴⁴, S.B. Silverstein^{147a}, V. Simak¹²⁷, O. Simard⁵, Lj. Simic^{13a}, S. Simion¹¹⁶, E. Simioni⁸², B. Simmons⁷⁷, R. Simoniello^{90a,90b}, M. Simonyan³⁶, P. Sinervo¹⁵⁹, N.B. Sinev¹¹⁵, V. Sipica¹⁴², G. Siragusa¹⁷⁵, A. Sircar⁷⁸, A.N. Sisakyan^{64,*}, S.Yu. Sivoklokov⁹⁸, J. Sjölin^{147a,147b}, T.B. Sjusen¹⁴, L.A. Skinnari¹⁵, H.P. Skottowe⁵⁷, K.Yu. Skovpen¹⁰⁸, P. Skubic¹¹², M. Slater¹⁸, T. Slavicek¹²⁷, K. Sliwa¹⁶², V. Smakhtin¹⁷³, B.H. Smart⁴⁶, L. Smestad¹¹⁸, S.Yu. Smirnov⁹⁷, Y. Smirnov⁹⁷, L.N. Smirnova^{98,ad}, O. Smirnova⁸⁰, K.M. Smith⁵³, M. Smizanska⁷¹, K. Smolek¹²⁷, A.A. Snesev⁹⁵, G. Snidero⁷⁵, J. Snow¹¹², S. Snyder²⁵, R. Sobie^{170,i}, F. Socher⁴⁴, J. Sodomka¹²⁷, A. Soffer¹⁵⁴, D.A. Soh^{152,s}, C.A. Solans³⁰, M. Solar¹²⁷, J. Solc¹²⁷, E.Yu. Soldatov⁹⁷, U. Soldevila¹⁶⁸,

E. Solfaroli Camillocci^{133a,133b}, A.A. Solodkov¹²⁹, O.V. Solovyanov¹²⁹, V. Solovyev¹²², P. Sommer⁴⁸, H.Y. Song^{33b}, N. Soni¹, A. Sood¹⁵, V. Sopko¹²⁷, B. Sopko¹²⁷, V. Sorin¹², M. Sosebee⁸, R. Soualah^{165a,165c}, P. Soueid⁹⁴, A.M. Soukharev¹⁰⁸, D. South⁴², S. Spagnolo^{72a,72b}, F. Spanò⁷⁶, W.R. Spearman⁵⁷, R. Spighi^{20a}, G. Spigo³⁰, M. Spousta¹²⁸, T. Spreitzer¹⁵⁹, B. Spurlock⁸, R.D. St. Denis⁵³, S. Staerz⁴⁴, J. Stahlman¹²¹, R. Stamen^{58a}, E. Stanecka³⁹, R.W. Stanek⁶, C. Stanescu^{135a}, M. Stanescu-Bellu⁴², M.M. Stanitzki⁴², S. Stapnes¹¹⁸, E.A. Starchenko¹²⁹, J. Stark⁵⁵, P. Starob¹²⁶, P. Starovoitov⁴², R. Staszewski³⁹, P. Stavina^{145a,*}, G. Steele⁵³, P. Steinberg²⁵, I. Stekl¹²⁷, B. Stelzer¹⁴³, H.J. Stelzer³⁰, O. Stelzer-Chilton^{160a}, H. Stenzel⁵², S. Stern¹⁰⁰, G.A. Stewart⁵³, J.A. Stillings²¹, M.C. Stockton⁸⁶, M. Stoebe⁸⁶, K. Stoerig⁴⁸, G. Stoicea^{26a}, P. Stolte⁵⁴, S. Stonjek¹⁰⁰, A.R. Stradling⁸, A. Straessner⁴⁴, J. Strandberg¹⁴⁸, S. Strandberg^{147a,147b}, A. Strandlie¹¹⁸, E. Strauss¹⁴⁴, M. Strauss¹¹², P. Strizenc^{145b}, R. Ströhmer¹⁷⁵, D.M. Strom¹¹⁵, R. Stroynowski⁴⁰, S.A. Stucci¹⁷, B. Stugu¹⁴, N.A. Styles⁴², D. Su¹⁴⁴, J. Su¹²⁴, H.S. Subramania³, R. Subramaniam⁷⁸, A. Succurro¹², Y. Sugaya¹¹⁷, C. Suhr¹⁰⁷, M. Suk¹²⁷, V.V. Sulin⁹⁵, S. Sultansoy^{4c}, T. Sumida⁶⁷, X. Sun^{33a}, J.E. Sundermann⁴⁸, K. Suruliz¹⁴⁰, G. Susinno^{37a,37b}, M.R. Sutton¹⁵⁰, Y. Suzuki⁶⁵, M. Svatos¹²⁶, S. Swedish¹⁶⁹, M. Swiatlowski¹⁴⁴, I. Sykora^{145a}, T. Sykora¹²⁸, D. Ta⁸⁹, K. Tackmann⁴², J. Taenzer¹⁵⁹, A. Taffard¹⁶⁴, R. Tafirout^{160a}, N. Taiblum¹⁵⁴, Y. Takahashi¹⁰², H. Takai²⁵, R. Takashima⁶⁸, H. Takeda⁶⁶, T. Takeshita¹⁴¹, Y. Takubo⁶⁵, M. Talby⁸⁴, A.A. Talyshev^{108,f}, J.Y.C. Tam¹⁷⁵, M.C. Tamsett^{78,ae}, K.G. Tan⁸⁷, J. Tanaka¹⁵⁶, R. Tanaka¹¹⁶, S. Tanaka¹³², S. Tanaka⁶⁵, A.J. Tanasijczuk¹⁴³, K. Tani⁶⁶, N. Tannoury⁸⁴, S. Tapprogge⁸², S. Tarem¹⁵³, F. Tarrade²⁹, G.F. Tartarelli^{90a}, P. Tas¹²⁸, M. Tasevsky¹²⁶, T. Tashiro⁶⁷, E. Tassi^{37a,37b}, A. Tavares Delgado^{125a,125b}, Y. Tayalati^{136d}, C. Taylor⁷⁷, F.E. Taylor⁹³, G.N. Taylor⁸⁷, W. Taylor^{160b}, F.A. Teischinger³⁰, M. Teixeira Dias Castanheira⁷⁵, P. Teixeira-Dias⁷⁶, K.K. Temming⁴⁸, H. Ten Kate³⁰, P.K. Teng¹⁵², S. Terada⁶⁵, K. Terashi¹⁵⁶, J. Terron⁸¹, S. Terzo¹⁰⁰, M. Testa⁴⁷, R.J. Teuscher^{159,i}, J. Therhaag²¹, T. Theveneaux-Pelzer³⁴, S. Thoma⁴⁸, J.P. Thomas¹⁸, J. Thomas-Wilsker⁷⁶, E.N. Thompson³⁵, P.D. Thompson¹⁸, P.D. Thompson¹⁵⁹, A.S. Thompson⁵³, L.A. Thomsen³⁶, E. Thomson¹²¹, M. Thomson²⁸, W.M. Thong⁸⁷, R.P. Thun^{88,*}, F. Tian³⁵, M.J. Tibbetts¹⁵, V.O. Tikhomirov^{95,af}, Yu.A. Tikhonov^{108,f}, S. Timoshenko⁹⁷, E. Tiouchichine⁸⁴, P. Tipton¹⁷⁷, S. Tisserant⁸⁴, T. Todorov⁵, S. Todorova-Nova¹²⁸, B. Toggerson¹⁶⁴, J. Tojo⁶⁹, S. Tokár^{145a}, K. Tokushuku⁶⁵, K. Tollefson⁸⁹, L. Tomlinson⁸³, M. Tomoto¹⁰², L. Tompkins³¹, K. Toms¹⁰⁴, N.D. Topilin⁶⁴, E. Torrence¹¹⁵, H. Torres¹⁴³, E. Torrò Pastor¹⁶⁸, J. Toth^{84,aa}, F. Touchard⁸⁴, D.R. Tovey¹⁴⁰, H.L. Tran¹¹⁶, T. Trefzger¹⁷⁵, L. Tremblet³⁰, A. Tricoli³⁰, I.M. Trigger^{160a}, S. Trincz-Duvoin⁷⁹, M.F. Tripiana⁷⁰, N. Triplett²⁵, W. Trischuk¹⁵⁹, B. Trocmé⁵⁵, C. Troncon^{90a}, M. Trottier-McDonald¹⁴³, M. Trovatelli^{135a,135b}, P. True⁸⁹, M. Trzebinski³⁹, A. Trzupek³⁹, C. Tsarouchas³⁰, J.C-L. Tseng¹¹⁹, P.V. Tsiarehshka⁹¹, D. Tsionou¹³⁷, G. Tsipolitis¹⁰, N. Tsirintanis⁹, S. Tsiskaridze¹², V. Tsiskaridze⁴⁸, E.G. Tskhadadze^{51a}, I.I. Tsukerman⁹⁶, V. Tsulaia¹⁵, S. Tsuno⁶⁵, D. Tsybychev¹⁴⁹, A. Tua¹⁴⁰, A. Tudorache^{26a}, V. Tudorache^{26a}, A.N. Tuna¹²¹, S.A. Tupputi^{20a,20b}, S. Turchikhin^{98,ad}, D. Turecek¹²⁷, I. Turk Cakir^{4d}, R. Turra^{90a,90b}, P.M. Tuts³⁵, A. Tykhonov⁷⁴, M. Tylmad^{147a,147b}, M. Tyndel¹³⁰, K. Uchida²¹, I. Ueda¹⁵⁶, R. Ueno²⁹, M. Ughetto⁸⁴, M. Uglan¹⁴, M. Uhlenbrock²¹, F. Ukegawa¹⁶¹, G. Unal³⁰, A. Undrus²⁵, G. Unel¹⁶⁴, F.C. Ungaro⁴⁸, Y. Unno⁶⁵, D. Urbaniec³⁵, P. Urquijo²¹, G. Usai⁸, A. Usanova⁶¹, L. Vacavant⁸⁴, V. Vacek¹²⁷, B. Vachon⁸⁶, N. Valencic¹⁰⁶, S. Valentinetti^{20a,20b}, A. Valero¹⁶⁸, L. Valery³⁴, S. Valkar¹²⁸, E. Valladolid Gallego¹⁶⁸, S. Vallecorsa⁴⁹, J.A. Valls Ferrer¹⁶⁸, R. Van Berg¹²¹, P.C. Van Der Deijl¹⁰⁶, R. van der Geer¹⁰⁶, H. van der Graaf¹⁰⁶, R. Van Der Leeuw¹⁰⁶, D. van der Ster³⁰, N. van Eldik³⁰, P. van Gemmeren⁶, J. Van Nieuwkoop¹⁴³, I. van Vulpen¹⁰⁶, M.C. van Woerden³⁰, M. Vanadia^{133a,133b}, W. Vandelli³⁰, A. Vaniachine⁶, P. Vankov⁴², F. Vannucci⁷⁹, G. Vardanyan¹⁷⁸, R. Vari^{133a}, E.W. Varnes⁷, T. Varol⁸⁵, D. Varouchas⁷⁹, A. Vartapetian⁸, K.E. Varvell¹⁵¹, V.I. Vassilikopoulos⁵⁶, F. Vazeille³⁴, T. Vazquez Schroeder⁵⁴, J. Veatch⁷, F. Veloso^{125a,125c}, S. Veneziano^{133a}, A. Ventura^{72a,72b}, D. Ventura⁸⁵, M. Venturi⁴⁸, N. Venturi¹⁵⁹, A. Venturini²³, V. Vercesi^{120a}, M. Verducci¹³⁹, W. Verkerke¹⁰⁶, J.C. Vermeulen¹⁰⁶, A. Vest⁴⁴, M.C. Vetterli^{143,d}, O. Viazlo⁸⁰, I. Vichou¹⁶⁶, T. Vickey^{146c,ag}, O.E. Vickey Boeriu^{146c}, G.H.A. Viehhauser¹¹⁹, S. Viel¹⁶⁹, R. Vigne³⁰, M. Villa^{20a,20b}, M. Villaplana Perez¹⁶⁸, E. Vilucchi⁴⁷, M.G. Vincter²⁹, V.B. Vinogradov⁶⁴, J. Virzi¹⁵, O. Vitells¹⁷³, I. Vivarelli¹⁵⁰, F. Vives Vaque³, S. Vlachos¹⁰, D. Vladoiu⁹⁹, M. Vlasak¹²⁷, A. Vogel²¹, P. Vokac¹²⁷, G. Volpi^{123a,123b}, M. Volpi⁸⁷, H. von der Schmitt¹⁰⁰, H. von Radziewski⁴⁸, E. von Toerne²¹, V. Vorobel¹²⁸, M. Vos¹⁶⁸, R. Voss³⁰, J.H. Vossebeld⁷³, N. Vranjes¹³⁷, M. Vranjes Milosavljevic¹⁰⁶, V. Vrba¹²⁶, M. Vreeswijk¹⁰⁶, T. Vu Anh⁴⁸, R. Vuillermet³⁰, I. Vukotic³¹, Z. Vykydal¹²⁷, W. Wagner¹⁷⁶, P. Wagner²¹, S. Wahrmund⁴⁴, J. Wakabayashi¹⁰², J. Walder⁷¹, R. Walker⁹⁹, W. Walkowiak¹⁴², R. Wall¹⁷⁷, P. Waller⁷³, B. Walsh¹⁷⁷, C. Wang^{152,ah}, C. Wang⁴⁵, F. Wang¹⁷⁴, H. Wang¹⁵, H. Wang⁴⁰, J. Wang⁴², J. Wang^{33a}, K. Wang⁸⁶, R. Wang¹⁰⁴, S.M. Wang¹⁵², T. Wang²¹, X. Wang¹⁷⁷, A. Warburton⁸⁶, C.P. Ward²⁸, D.R. Wardrope⁷⁷, M. Warsinsky⁴⁸, A. Washbrook⁴⁶, C. Wasicki⁴², I. Watanabe⁶⁶, P.M. Watkins¹⁸, A.T. Watson¹⁸, I.J. Watson¹⁵¹, M.F. Watson¹⁸, G. Watts¹³⁹, S. Watts⁸³, B.M. Waugh⁷⁷, S. Webb⁸³, M.S. Weber¹⁷, S.W. Weber¹⁷⁵, J.S. Webster³¹, A.R. Weidberg¹¹⁹, P. Weigell¹⁰⁰, B. Weinert⁶⁰, J. Weingarten⁵⁴, C. Weiser⁴⁸, H. Weits¹⁰⁶, P.S. Wells³⁰, T. Wenaus²⁵, D. Wendland¹⁶, Z. Weng^{152,s}, T. Wengler³⁰, S. Wenig³⁰, N. Vermes²¹, M. Werner⁴⁸, P. Werner³⁰, M. Wessels^{58a}, J. Wetter¹⁶², K. Whalen²⁹, A. White⁸, M.J. White¹, R. White^{32b}, S. White^{123a,123b}, D. Whiteson¹⁶⁴, D. Wicke¹⁷⁶, F.J. Wickens¹³⁰, W. Wiedenmann¹⁷⁴, M. Wielers¹³⁰, P. Wienemann²¹, C. Wiglesworth³⁶,

L.A.M. Wiik-Fuchs²¹, P.A. Wijeratne⁷⁷, A. Wildauer¹⁰⁰, M.A. Wildt^{42,ai}, H.G. Wilkens³⁰, J.Z. Will⁹⁹, H.H. Williams¹²¹, S. Williams²⁸, C. Willis⁸⁹, S. Willocq⁸⁵, J.A. Wilson¹⁸, A. Wilson⁸⁸, I. Wingerter-Seez⁵, S. Winkelmann⁴⁸, F. Winklmeier¹¹⁵, M. Wittgen¹⁴⁴, T. Wittig⁴³, J. Wittkowski⁹⁹, S.J. Wollstadt⁸², M.W. Wolter³⁹, H. Wolters^{125a,125c}, B.K. Wosiek³⁹, J. Wotschack³⁰, M.J. Woudstra⁸³, K.W. Wozniak³⁹, M. Wright⁵³, S.L. Wu¹⁷⁴, X. Wu⁴⁹, Y. Wu⁸⁸, E. Wulf³⁵, T.R. Wyatt⁸³, B.M. Wynne⁴⁶, S. Xella³⁶, M. Xiao¹³⁷, D. Xu^{33a}, L. Xu^{33b,aj}, B. Yabsley¹⁵¹, S. Yacoob^{146b,ak}, M. Yamada⁶⁵, H. Yamaguchi¹⁵⁶, Y. Yamaguchi¹⁵⁶, A. Yamamoto⁶⁵, K. Yamamoto⁶³, S. Yamamoto¹⁵⁶, T. Yamamura¹⁵⁶, T. Yamanaka¹⁵⁶, K. Yamauchi¹⁰², Y. Yamazaki⁶⁶, Z. Yan²², H. Yang^{33e}, H. Yang¹⁷⁴, U.K. Yang⁸³, Y. Yang¹¹⁰, S. Yanush⁹², L. Yao^{33a}, W-M. Yao¹⁵, Y. Yasu⁶⁵, E. Yatsenko⁴², K.H. Yau Wong²¹, J. Ye⁴⁰, S. Ye²⁵, A.L. Yen⁵⁷, E. Yildirim⁴², M. Yilmaz^{4b}, R. Yoosofmiya¹²⁴, K. Yorita¹⁷², R. Yoshida⁶, K. Yoshihara¹⁵⁶, C. Young¹⁴⁴, C.J.S. Young³⁰, S. Youssef²², D.R. Yu¹⁵, J. Yu⁸, J.M. Yu⁸⁸, J. Yu¹¹³, L. Yuan⁶⁶, A. Yurkewicz¹⁰⁷, B. Zabinski³⁹, R. Zaidan⁶², A.M. Zaitsev^{129,x}, A. Zaman¹⁴⁹, S. Zambito²³, L. Zanello^{133a,133b}, D. Zanzi¹⁰⁰, A. Zaytsev²⁵, C. Zeitnitz¹⁷⁶, M. Zeman¹²⁷, A. Zemla^{38a}, K. Zengel²³, O. Zenin¹²⁹, T. Ženiš^{145a}, D. Zerwas¹¹⁶, G. Zevi della Porta⁵⁷, D. Zhang⁸⁸, F. Zhang¹⁷⁴, H. Zhang⁸⁹, J. Zhang⁶, L. Zhang¹⁵², X. Zhang^{33d}, Z. Zhang¹¹⁶, Z. Zhao^{33b}, A. Zhemchugov⁶⁴, J. Zhong¹¹⁹, B. Zhou⁸⁸, L. Zhou³⁵, N. Zhou¹⁶⁴, C.G. Zhu^{33d}, H. Zhu^{33a}, J. Zhu⁸⁸, Y. Zhu^{33b}, X. Zhuang^{33a}, A. Zibell⁹⁹, D. Ziemska⁶⁰, N.I. Zimine⁶⁴, C. Zimmermann⁸², R. Zimmermann²¹, S. Zimmermann²¹, S. Zimmermann⁴⁸, Z. Zinonos⁵⁴, M. Ziolkowski¹⁴², R. Zitoun⁵, G. Zobernig¹⁷⁴, A. Zoccoli^{20a,20b}, M. zur Nedden¹⁶, G. Zurzolo^{103a,103b}, V. Zutshi¹⁰⁷, L. Zwalinski³⁰.

¹ Department of Physics, University of Adelaide, Adelaide, Australia

² Physics Department, SUNY Albany, Albany NY, United States of America

³ Department of Physics, University of Alberta, Edmonton AB, Canada

⁴ (a) Department of Physics, Ankara University, Ankara; (b) Department of Physics, Gazi University, Ankara; (c) Division of Physics, TOBB University of Economics and Technology, Ankara; (d) Turkish Atomic Energy Authority, Ankara, Turkey

⁵ LAPP, CNRS/IN2P3 and Université de Savoie, Annecy-le-Vieux, France

⁶ High Energy Physics Division, Argonne National Laboratory, Argonne IL, United States of America

⁷ Department of Physics, University of Arizona, Tucson AZ, United States of America

⁸ Department of Physics, The University of Texas at Arlington, Arlington TX, United States of America

⁹ Physics Department, University of Athens, Athens, Greece

¹⁰ Physics Department, National Technical University of Athens, Zografou, Greece

¹¹ Institute of Physics, Azerbaijan Academy of Sciences, Baku, Azerbaijan

¹² Institut de Física d'Altes Energies and Departament de Física de la Universitat Autònoma de Barcelona, Barcelona, Spain

¹³ (a) Institute of Physics, University of Belgrade, Belgrade; (b) Vinca Institute of Nuclear Sciences, University of Belgrade, Belgrade, Serbia

¹⁴ Department for Physics and Technology, University of Bergen, Bergen, Norway

¹⁵ Physics Division, Lawrence Berkeley National Laboratory and University of California, Berkeley CA, United States of America

¹⁶ Department of Physics, Humboldt University, Berlin, Germany

¹⁷ Albert Einstein Center for Fundamental Physics and Laboratory for High Energy Physics, University of Bern, Bern, Switzerland

¹⁸ School of Physics and Astronomy, University of Birmingham, Birmingham, United Kingdom

¹⁹ (a) Department of Physics, Bogazici University, Istanbul; (b) Department of Physics, Dogus University, Istanbul;

(c) Department of Physics Engineering, Gaziantep University, Gaziantep, Turkey

²⁰ (a) INFN Sezione di Bologna; (b) Dipartimento di Fisica e Astronomia, Università di Bologna, Bologna, Italy

²¹ Physikalisches Institut, University of Bonn, Bonn, Germany

²² Department of Physics, Boston University, Boston MA, United States of America

²³ Department of Physics, Brandeis University, Waltham MA, United States of America

²⁴ (a) Universidade Federal do Rio De Janeiro COPPE/EE/IF, Rio de Janeiro; (b) Federal University of Juiz de Fora (UFJF), Juiz de Fora; (c) Federal University of Sao Joao del Rei (UFSJ), Sao Joao del Rei; (d) Instituto de Fisica, Universidade de Sao Paulo, Sao Paulo, Brazil

²⁵ Physics Department, Brookhaven National Laboratory, Upton NY, United States of America

²⁶ (a) National Institute of Physics and Nuclear Engineering, Bucharest; (b) National Institute for Research and Development of Isotopic and Molecular Technologies, Physics Department, Cluj Napoca; (c) University Politehnica Bucharest, Bucharest; (d) West University in Timisoara, Timisoara, Romania

²⁷ Departamento de Física, Universidad de Buenos Aires, Buenos Aires, Argentina

²⁸ Cavendish Laboratory, University of Cambridge, Cambridge, United Kingdom

²⁹ Department of Physics, Carleton University, Ottawa ON, Canada

- ³⁰ CERN, Geneva, Switzerland
- ³¹ Enrico Fermi Institute, University of Chicago, Chicago IL, United States of America
- ³² ^(a) Departamento de Física, Pontificia Universidad Católica de Chile, Santiago; ^(b) Departamento de Física, Universidad Técnica Federico Santa María, Valparaíso, Chile
- ³³ ^(a) Institute of High Energy Physics, Chinese Academy of Sciences, Beijing; ^(b) Department of Modern Physics, University of Science and Technology of China, Anhui; ^(c) Department of Physics, Nanjing University, Jiangsu; ^(d) School of Physics, Shandong University, Shandong; ^(e) Physics Department, Shanghai Jiao Tong University, Shanghai, China
- ³⁴ Laboratoire de Physique Corpusculaire, Clermont Université and Université Blaise Pascal and CNRS/IN2P3, Clermont-Ferrand, France
- ³⁵ Nevis Laboratory, Columbia University, Irvington NY, United States of America
- ³⁶ Niels Bohr Institute, University of Copenhagen, Kobenhavn, Denmark
- ³⁷ ^(a) INFN Gruppo Collegato di Cosenza, Laboratori Nazionali di Frascati; ^(b) Dipartimento di Fisica, Università della Calabria, Rende, Italy
- ³⁸ ^(a) AGH University of Science and Technology, Faculty of Physics and Applied Computer Science, Krakow; ^(b) Marian Smoluchowski Institute of Physics, Jagiellonian University, Krakow, Poland
- ³⁹ The Henryk Niewodniczanski Institute of Nuclear Physics, Polish Academy of Sciences, Krakow, Poland
- ⁴⁰ Physics Department, Southern Methodist University, Dallas TX, United States of America
- ⁴¹ Physics Department, University of Texas at Dallas, Richardson TX, United States of America
- ⁴² DESY, Hamburg and Zeuthen, Germany
- ⁴³ Institut für Experimentelle Physik IV, Technische Universität Dortmund, Dortmund, Germany
- ⁴⁴ Institut für Kern- und Teilchenphysik, Technische Universität Dresden, Dresden, Germany
- ⁴⁵ Department of Physics, Duke University, Durham NC, United States of America
- ⁴⁶ SUPA - School of Physics and Astronomy, University of Edinburgh, Edinburgh, United Kingdom
- ⁴⁷ INFN Laboratori Nazionali di Frascati, Frascati, Italy
- ⁴⁸ Fakultät für Mathematik und Physik, Albert-Ludwigs-Universität, Freiburg, Germany
- ⁴⁹ Section de Physique, Université de Genève, Geneva, Switzerland
- ⁵⁰ ^(a) INFN Sezione di Genova; ^(b) Dipartimento di Fisica, Università di Genova, Genova, Italy
- ⁵¹ ^(a) E. Andronikashvili Institute of Physics, Iv. Javakishvili Tbilisi State University, Tbilisi; ^(b) High Energy Physics Institute, Tbilisi State University, Tbilisi, Georgia
- ⁵² II Physikalisches Institut, Justus-Liebig-Universität Giessen, Giessen, Germany
- ⁵³ SUPA - School of Physics and Astronomy, University of Glasgow, Glasgow, United Kingdom
- ⁵⁴ II Physikalisches Institut, Georg-August-Universität, Göttingen, Germany
- ⁵⁵ Laboratoire de Physique Subatomique et de Cosmologie, Université Grenoble-Alpes, CNRS/IN2P3, Grenoble, France
- ⁵⁶ Department of Physics, Hampton University, Hampton VA, United States of America
- ⁵⁷ Laboratory for Particle Physics and Cosmology, Harvard University, Cambridge MA, United States of America
- ⁵⁸ ^(a) Kirchoff-Institut für Physik, Ruprecht-Karls-Universität Heidelberg, Heidelberg; ^(b) Physikalisches Institut, Ruprecht-Karls-Universität Heidelberg, Heidelberg; ^(c) ZITI Institut für technische Informatik, Ruprecht-Karls-Universität Heidelberg, Mannheim, Germany
- ⁵⁹ Faculty of Applied Information Science, Hiroshima Institute of Technology, Hiroshima, Japan
- ⁶⁰ Department of Physics, Indiana University, Bloomington IN, United States of America
- ⁶¹ Institut für Astro- und Teilchenphysik, Leopold-Franzens-Universität, Innsbruck, Austria
- ⁶² University of Iowa, Iowa City IA, United States of America
- ⁶³ Department of Physics and Astronomy, Iowa State University, Ames IA, United States of America
- ⁶⁴ Joint Institute for Nuclear Research, JINR Dubna, Dubna, Russia
- ⁶⁵ KEK, High Energy Accelerator Research Organization, Tsukuba, Japan
- ⁶⁶ Graduate School of Science, Kobe University, Kobe, Japan
- ⁶⁷ Faculty of Science, Kyoto University, Kyoto, Japan
- ⁶⁸ Kyoto University of Education, Kyoto, Japan
- ⁶⁹ Department of Physics, Kyushu University, Fukuoka, Japan
- ⁷⁰ Instituto de Física La Plata, Universidad Nacional de La Plata and CONICET, La Plata, Argentina
- ⁷¹ Physics Department, Lancaster University, Lancaster, United Kingdom
- ⁷² ^(a) INFN Sezione di Lecce; ^(b) Dipartimento di Matematica e Fisica, Università del Salento, Lecce, Italy
- ⁷³ Oliver Lodge Laboratory, University of Liverpool, Liverpool, United Kingdom
- ⁷⁴ Department of Physics, Jožef Stefan Institute and University of Ljubljana, Ljubljana, Slovenia
- ⁷⁵ School of Physics and Astronomy, Queen Mary University of London, London, United Kingdom
- ⁷⁶ Department of Physics, Royal Holloway University of London, Surrey, United Kingdom

- 77 Department of Physics and Astronomy, University College London, London, United Kingdom
- 78 Louisiana Tech University, Ruston LA, United States of America
- 79 Laboratoire de Physique Nucléaire et de Hautes Energies, UPMC and Université Paris-Diderot and CNRS/IN2P3, Paris, France
- 80 Fysiska institutionen, Lunds universitet, Lund, Sweden
- 81 Departamento de Física Teórica C-15, Universidad Autonoma de Madrid, Madrid, Spain
- 82 Institut für Physik, Universität Mainz, Mainz, Germany
- 83 School of Physics and Astronomy, University of Manchester, Manchester, United Kingdom
- 84 CPPM, Aix-Marseille Université and CNRS/IN2P3, Marseille, France
- 85 Department of Physics, University of Massachusetts, Amherst MA, United States of America
- 86 Department of Physics, McGill University, Montreal QC, Canada
- 87 School of Physics, University of Melbourne, Victoria, Australia
- 88 Department of Physics, The University of Michigan, Ann Arbor MI, United States of America
- 89 Department of Physics and Astronomy, Michigan State University, East Lansing MI, United States of America
- 90 ^(a) INFN Sezione di Milano; ^(b) Dipartimento di Fisica, Università di Milano, Milano, Italy
- 91 B.I. Stepanov Institute of Physics, National Academy of Sciences of Belarus, Minsk, Republic of Belarus
- 92 National Scientific and Educational Centre for Particle and High Energy Physics, Minsk, Republic of Belarus
- 93 Department of Physics, Massachusetts Institute of Technology, Cambridge MA, United States of America
- 94 Group of Particle Physics, University of Montreal, Montreal QC, Canada
- 95 P.N. Lebedev Institute of Physics, Academy of Sciences, Moscow, Russia
- 96 Institute for Theoretical and Experimental Physics (ITEP), Moscow, Russia
- 97 Moscow Engineering and Physics Institute (MEPhI), Moscow, Russia
- 98 D.V.Skobeltzyn Institute of Nuclear Physics, M.V.Lomonosov Moscow State University, Moscow, Russia
- 99 Fakultät für Physik, Ludwig-Maximilians-Universität München, München, Germany
- 100 Max-Planck-Institut für Physik (Werner-Heisenberg-Institut), München, Germany
- 101 Nagasaki Institute of Applied Science, Nagasaki, Japan
- 102 Graduate School of Science and Kobayashi-Maskawa Institute, Nagoya University, Nagoya, Japan
- 103 ^(a) INFN Sezione di Napoli; ^(b) Dipartimento di Fisica, Università di Napoli, Napoli, Italy
- 104 Department of Physics and Astronomy, University of New Mexico, Albuquerque NM, United States of America
- 105 Institute for Mathematics, Astrophysics and Particle Physics, Radboud University Nijmegen/Nikhef, Nijmegen, Netherlands
- 106 Nikhef National Institute for Subatomic Physics and University of Amsterdam, Amsterdam, Netherlands
- 107 Department of Physics, Northern Illinois University, DeKalb IL, United States of America
- 108 Budker Institute of Nuclear Physics, SB RAS, Novosibirsk, Russia
- 109 Department of Physics, New York University, New York NY, United States of America
- 110 Ohio State University, Columbus OH, United States of America
- 111 Faculty of Science, Okayama University, Okayama, Japan
- 112 Homer L. Dodge Department of Physics and Astronomy, University of Oklahoma, Norman OK, United States of America
- 113 Department of Physics, Oklahoma State University, Stillwater OK, United States of America
- 114 Palacký University, RCPTM, Olomouc, Czech Republic
- 115 Center for High Energy Physics, University of Oregon, Eugene OR, United States of America
- 116 LAL, Université Paris-Sud and CNRS/IN2P3, Orsay, France
- 117 Graduate School of Science, Osaka University, Osaka, Japan
- 118 Department of Physics, University of Oslo, Oslo, Norway
- 119 Department of Physics, Oxford University, Oxford, United Kingdom
- 120 ^(a) INFN Sezione di Pavia; ^(b) Dipartimento di Fisica, Università di Pavia, Pavia, Italy
- 121 Department of Physics, University of Pennsylvania, Philadelphia PA, United States of America
- 122 Petersburg Nuclear Physics Institute, Gatchina, Russia
- 123 ^(a) INFN Sezione di Pisa; ^(b) Dipartimento di Fisica E. Fermi, Università di Pisa, Pisa, Italy
- 124 Department of Physics and Astronomy, University of Pittsburgh, Pittsburgh PA, United States of America
- 125 ^(a) Laboratorio de Instrumentacao e Fisica Experimental de Particulas - LIP, Lisboa; ^(b) Faculdade de Ciências, Universidade de Lisboa, Lisboa; ^(c) Department of Physics, University of Coimbra, Coimbra; ^(d) Centro de Física Nuclear da Universidade de Lisboa, Lisboa; ^(e) Departamento de Física, Universidade do Minho, Braga; ^(f) Departamento de Física Teórica y del Cosmos and CAFPE, Universidad de Granada, Granada (Spain); ^(g) Dep Física and CEFITEC of Faculdade de Ciências e Tecnologia, Universidade Nova de Lisboa, Caparica, Portugal
- 126 Institute of Physics, Academy of Sciences of the Czech Republic, Praha, Czech Republic
- 127 Czech Technical University in Prague, Praha, Czech Republic

- 128 Faculty of Mathematics and Physics, Charles University in Prague, Praha, Czech Republic
 129 State Research Center Institute for High Energy Physics, Protvino, Russia
 130 Particle Physics Department, Rutherford Appleton Laboratory, Didcot, United Kingdom
 131 Physics Department, University of Regina, Regina SK, Canada
 132 Ritsumeikan University, Kusatsu, Shiga, Japan
 133 ^(a) INFN Sezione di Roma; ^(b) Dipartimento di Fisica, Sapienza Università di Roma, Roma, Italy
 134 ^(a) INFN Sezione di Roma Tor Vergata; ^(b) Dipartimento di Fisica, Università di Roma Tor Vergata, Roma, Italy
 135 ^(a) INFN Sezione di Roma Tre; ^(b) Dipartimento di Matematica e Fisica, Università Roma Tre, Roma, Italy
 136 ^(a) Faculté des Sciences Ain Chock, Réseau Universitaire de Physique des Hautes Energies - Université Hassan II, Casablanca; ^(b) Centre National de l'Énergie des Sciences Techniques Nucleaires, Rabat; ^(c) Faculté des Sciences Semlalia, Université Cadi Ayyad, LPHEA-Marrakech; ^(d) Faculté des Sciences, Université Mohamed Premier and LPTPM, Oujda; ^(e) Faculté des sciences, Université Mohammed V-Agdal, Rabat, Morocco
 137 DSM/IRFU (Institut de Recherches sur les Lois Fondamentales de l'Univers), CEA Saclay (Commissariat à l'Énergie Atomique et aux Énergies Alternatives), Gif-sur-Yvette, France
 138 Santa Cruz Institute for Particle Physics, University of California Santa Cruz, Santa Cruz CA, United States of America
 139 Department of Physics, University of Washington, Seattle WA, United States of America
 140 Department of Physics and Astronomy, University of Sheffield, Sheffield, United Kingdom
 141 Department of Physics, Shinshu University, Nagano, Japan
 142 Fachbereich Physik, Universität Siegen, Siegen, Germany
 143 Department of Physics, Simon Fraser University, Burnaby BC, Canada
 144 SLAC National Accelerator Laboratory, Stanford CA, United States of America
 145 ^(a) Faculty of Mathematics, Physics & Informatics, Comenius University, Bratislava; ^(b) Department of Subnuclear Physics, Institute of Experimental Physics of the Slovak Academy of Sciences, Kosice, Slovak Republic
 146 ^(a) Department of Physics, University of Cape Town, Cape Town; ^(b) Department of Physics, University of Johannesburg, Johannesburg; ^(c) School of Physics, University of the Witwatersrand, Johannesburg, South Africa
 147 ^(a) Department of Physics, Stockholm University; ^(b) The Oskar Klein Centre, Stockholm, Sweden
 148 Physics Department, Royal Institute of Technology, Stockholm, Sweden
 149 Departments of Physics & Astronomy and Chemistry, Stony Brook University, Stony Brook NY, United States of America
 150 Department of Physics and Astronomy, University of Sussex, Brighton, United Kingdom
 151 School of Physics, University of Sydney, Sydney, Australia
 152 Institute of Physics, Academia Sinica, Taipei, Taiwan
 153 Department of Physics, Technion: Israel Institute of Technology, Haifa, Israel
 154 Raymond and Beverly Sackler School of Physics and Astronomy, Tel Aviv University, Tel Aviv, Israel
 155 Department of Physics, Aristotle University of Thessaloniki, Thessaloniki, Greece
 156 International Center for Elementary Particle Physics and Department of Physics, The University of Tokyo, Tokyo, Japan
 157 Graduate School of Science and Technology, Tokyo Metropolitan University, Tokyo, Japan
 158 Department of Physics, Tokyo Institute of Technology, Tokyo, Japan
 159 Department of Physics, University of Toronto, Toronto ON, Canada
 160 ^(a) TRIUMF, Vancouver BC; ^(b) Department of Physics and Astronomy, York University, Toronto ON, Canada
 161 Faculty of Pure and Applied Sciences, University of Tsukuba, Tsukuba, Japan
 162 Department of Physics and Astronomy, Tufts University, Medford MA, United States of America
 163 Centro de Investigaciones, Universidad Antonio Narino, Bogota, Colombia
 164 Department of Physics and Astronomy, University of California Irvine, Irvine CA, United States of America
 165 ^(a) INFN Gruppo Collegato di Udine, Sezione di Trieste, Udine; ^(b) ICTP, Trieste; ^(c) Dipartimento di Chimica, Fisica e Ambiente, Università di Udine, Udine, Italy
 166 Department of Physics, University of Illinois, Urbana IL, United States of America
 167 Department of Physics and Astronomy, University of Uppsala, Uppsala, Sweden
 168 Instituto de Física Corpuscular (IFIC) and Departamento de Física Atómica, Molecular y Nuclear and Departamento de Ingeniería Electrónica and Instituto de Microelectrónica de Barcelona (IMB-CNM), University of Valencia and CSIC, Valencia, Spain
 169 Department of Physics, University of British Columbia, Vancouver BC, Canada
 170 Department of Physics and Astronomy, University of Victoria, Victoria BC, Canada
 171 Department of Physics, University of Warwick, Coventry, United Kingdom
 172 Waseda University, Tokyo, Japan
 173 Department of Particle Physics, The Weizmann Institute of Science, Rehovot, Israel

- 174 Department of Physics, University of Wisconsin, Madison WI, United States of America
 175 Fakultät für Physik und Astronomie, Julius-Maximilians-Universität, Würzburg, Germany
 176 Fachbereich C Physik, Bergische Universität Wuppertal, Wuppertal, Germany
 177 Department of Physics, Yale University, New Haven CT, United States of America
 178 Yerevan Physics Institute, Yerevan, Armenia
 179 Centre de Calcul de l'Institut National de Physique Nucléaire et de Physique des Particules (IN2P3),
 Villeurbanne, France
- ^a Also at Department of Physics, King's College London, London, United Kingdom
^b Also at Institute of Physics, Azerbaijan Academy of Sciences, Baku, Azerbaijan
^c Also at Particle Physics Department, Rutherford Appleton Laboratory, Didcot, United Kingdom
^d Also at TRIUMF, Vancouver BC, Canada
^e Also at Department of Physics, California State University, Fresno CA, United States of America
^f Also at Novosibirsk State University, Novosibirsk, Russia
^g Also at CPPM, Aix-Marseille Université and CNRS/IN2P3, Marseille, France
^h Also at Università di Napoli Parthenope, Napoli, Italy
ⁱ Also at Institute of Particle Physics (IPP), Canada
^j Also at Department of Physics, St. Petersburg State Polytechnical University, St. Petersburg, Russia
^k Also at Department of Financial and Management Engineering, University of the Aegean, Chios, Greece
^l Also at Louisiana Tech University, Ruston LA, United States of America
^m Also at Institutio Catalana de Recerca i Estudis Avancats, ICREA, Barcelona, Spain
ⁿ Also at CERN, Geneva, Switzerland
^o Also at Ochadai Academic Production, Ochanomizu University, Tokyo, Japan
^p Also at Manhattan College, New York NY, United States of America
^q Also at Institute of Physics, Academia Sinica, Taipei, Taiwan
^r Also at LAL, Université Paris-Sud and CNRS/IN2P3, Orsay, France
^s Also at School of Physics and Engineering, Sun Yat-sen University, Guangzhou, China
^t Also at Academia Sinica Grid Computing, Institute of Physics, Academia Sinica, Taipei, Taiwan
^u Also at Laboratoire de Physique Nucléaire et de Hautes Energies, UPMC and Université Paris-Diderot and
 CNRS/IN2P3, Paris, France
^v Also at School of Physical Sciences, National Institute of Science Education and Research, Bhubaneswar, India
^w Also at Dipartimento di Fisica, Sapienza Università di Roma, Roma, Italy
^x Also at Moscow Institute of Physics and Technology State University, Dolgoprudny, Russia
^y Also at Section de Physique, Université de Genève, Geneva, Switzerland
^z Also at Department of Physics, The University of Texas at Austin, Austin TX, United States of America
^{aa} Also at Institute for Particle and Nuclear Physics, Wigner Research Centre for Physics, Budapest, Hungary
^{ab} Also at International School for Advanced Studies (SISSA), Trieste, Italy
^{ac} Also at Department of Physics and Astronomy, University of South Carolina, Columbia SC, United States of
 America
^{ad} Also at Faculty of Physics, M.V.Lomonosov Moscow State University, Moscow, Russia
^{ae} Also at Physics Department, Brookhaven National Laboratory, Upton NY, United States of America
^{af} Also at Moscow Engineering and Physics Institute (MEPhI), Moscow, Russia
^{ag} Also at Department of Physics, Oxford University, Oxford, United Kingdom
^{ah} Also at Department of Physics, Nanjing University, Jiangsu, China
^{ai} Also at Institut für Experimentalphysik, Universität Hamburg, Hamburg, Germany
^{aj} Also at Department of Physics, The University of Michigan, Ann Arbor MI, United States of America
^{ak} Also at Discipline of Physics, University of KwaZulu-Natal, Durban, South Africa
- * Deceased